J.H.R. Ietswaart

Modelling the Segregation Mechanism of low copy number Plasmid pB171

Masters thesis, June 30^{th} 2011

Primary Supervisor:
Prof.dr. M. Howard

Secondary Supervisor:
Prof.dr. H. Schiessel

Instituut Lorentz, Universiteit Leiden
John Innes Centre

Contents

Abstract

Often low copy number plasmids in bacterial cells exhibit active mechanisms to ensure stable inheritance. In this master thesis we investigate several models that aim to explain the equidistant positioning of pB171 plasmids in *E. coli*. In this system a walker type ATPase, ParA, forms filamentous structures on the nucleoid. Plasmids with attached ParB, a DNA binding protein, follow the retractive movement of ParA [1]. We show that a polymer pulling model in which the plasmid detachment rate depends critically on the plasmid bound ParB levels can generate partitioning. Furthermore a recently proposed biased diffusion model [2] in which the plasmid diffusion is influenced by the dynamic ParA concentration can direct motion towards mid cell. However the necessity of a high plasmid diffusion constant renders it unlikely to be the actual mechanism used by bacteria. A slight variation of this idea where diffusing oligomers pull on plasmids encounters the same problems as a biased diffusion model. The influence of polymer drag which depends on the length of the filament can be beneficial though it seems unlikely to be the sole mechanism to partition plasmids. Finally, in our favoured model we show that ParA polymers can position plasmids equidistantly with the assumption that ParA subunits bind along the filament and slide to the tip end, thereby influencing the polymerization rate critically.

1 Introduction

In all living organisms stable DNA inheritance is crucial to proliferation. Cells have evolved many intricate processes to ensure that the genome is accurately moved and positioned from parent to daughter cells. In prokaryotes genetic material comes in multiple ways. Most common are chromosomal DNA and plasmids. Plasmids are double strands and relatively short ($\sim 1 - 10^3$ kilobasebairs (kbp)) compared to the chromosome (4.6Mbp in *E. coli*) that can replicate independently from the chromosome [3]. Both forms have their own distinct mechanisms to ensure partitioning of DNA. Some plasmids only occur in low copy number ($\sim 1 - 10$) and they exhibit active segregation mechanism that requires only three components: a centromere-like DNA site, an NTPase and a DNA binding protein [4]. Therefore they represent good model systems to study segregation of genetic material.

In general bacterial DNA partitioning mechanisms are divided into three classes depending on the structure of the NTPase. Type I contain a Walker box ATPase, ParA. Type II systems use an actin homologue called ParM and only recently type III was defined with the discovery of a tubulin-like GTPase TubZ. Both actin and microtubule dynamics have been extensively studied in eukaryotes, but the mechanism by which ParA exerts force on DNA to ensure segregation remains elusive. Various type I ParAs exhibit seemingly distinct features and it is thought that there are several slight variations in type I DNA segregation mechanisms. MinD, also a Walker type ATPase is known to be involved in bacterial cell division [5].

Type I *par* systems are further classified depending on whether the ParA protein contains an extra N-terminal of approximately 100 residues (type Ia) that are not found in type Ib proteins. These type Ia ParAs act as an autorepressor of *par* protein transcription [6]. Whether this distinction implies different segregation mechanisms is still under debate as there is experimental evidence that a type Ib ParA protein named PpfA involved in the partitioning of chemotaxis clusters in *Rhodobacter sphaeroides*, exhibits close resemblance to the particular type Ia ParA of plasmid P1 in *E. coli* [7] [8]. Also present in *E. coli* is the

low copy number plasmid pB171 (69kbp), encoding for virulence factors [9] and exhibiting two separate partitioning mechanisms. The *par1* locus is responsible for a well characterized type II system [4], but the adjacent *par2* locus allows for type Ib segregation. The precise mechanism for the type Ib partitioning is currently unclear. This master thesis investigates by means of theoretical analysis and computer simulations whether various possible segregation mechanisms lead to *par2* plasmid partitioning of plasmid pB171 as observed in experiments.

The *par2* locus contains the two adjacent genes *parA* and *parB*, as well as the regions immediately upstream (*parC1*) and downstream (*parC2*) of them[9]. ParB is the second component of this segregation mechanism: the DNA binding protein. Both ParA and ParB form dimers *in vivo* and subsequently when we refer to a ParA (or ParB) (sub)unit, we mean a $ParA_2$ or $ParB_2$ dimer. ParB units bind to both *parC1* and *parC2* as they exhibit respectively 17 and 18 binding sites [10] [11]. By binding *parC1* ParB autorepresses the transcription of the *parAB* operon. Since the type Ia P1 plasmid segregation mechanism in *E. coli* and type Ib chemotaxis cluster positioning in *Rhodobacter sphaeroides* appear similar but not identical to the *par2* system we assess also experimental facts from these systems. In *Rhodobacter* the cluster plays the role of plasmid that needs stabilization. In cells without a cluster due a defective segregation mechanism chemotaxis is disrupted[12].

In vivo ParA forms helical structures extending to the ends of the nucleoid, the region inside a cell where the chromosomal DNA is located [13]. P1 (ParA-ATP)$_2$ but not (ParA-ADP)$_2$ binds DNA sequence independently *in vitro* [2]. In presence of both ParB and *parC1/parC2* ParA oscillates in these spiral shaped structures [13]. Mutations in the Walker motif of ParA abolishes both oscillations and plasmid positioning. Similar defects in P1 ParA impair DNA binding [2], which indicates that ParA binding to DNA is necessary for ParA oscillations and plasmid positioning. In chemotaxis cluster positioning PpfA monomers do not bind the nucleoid and ATP hydrolysis is necessary for cluster segregation but not for nucleoid binding of (PpfA-ATP)$_2$. In P1 *in vitro* the binding of ATP and attainment of potency for (ParA-ATP)$_2$ to bind DNA is a rate limit-

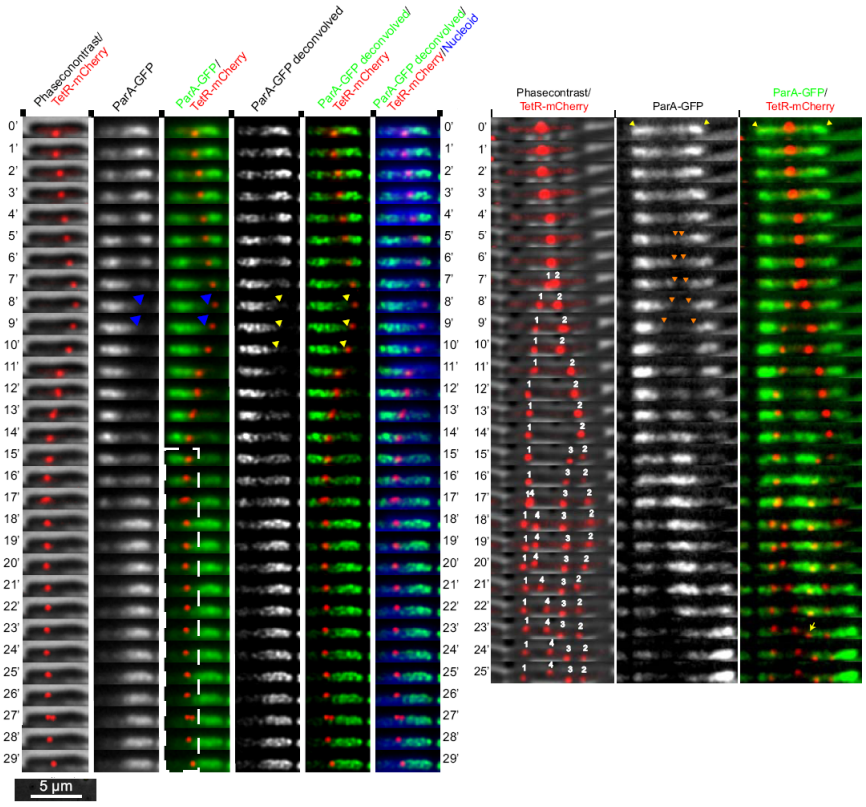

Figure 1: Typical kymographs of 29 (left) and 25 (right) minutes in which ParA-GFP(green) extends towards a plasmid, but upon attachment (e.g. at the blue and yellow arrows) initiates retraction. The plasmid (with inserted DNA binding site for Tetr-mCherry shown in red) follows the retracting ParA until a newly formed, opposing filament catches up. In effect this can lead to oscillations (left) and segregation of plasmids (right) after duplication. The nucleoid is stained with Hoechst (blue) [1].

ing step that takes $20-50s$. Since cytoplasmic diffusion of proteins is estimated to be $8\mu m^2/s$ [14] this indicates that this time period is long enough to induce a uniform cytoplasmic distribution of the ATP bound form of ParA. ParA and ParB interact in two hybrid assays[15] and it turns out that ParB stimulates the ATPase activity of ParA via its N terminus [1]. This suggests that varying ParB concentrations can influence the concentration of nucleoid bound ParA.

Both pB171 and P1 ParA polymerize *in vitro* in the presence of ATP [15][6]

and pB171 ParB stimulates further ParA polymerization [16], but whether these facts are also true *in vivo* remains to be seen. Interestingly, both P1 ParA and PpfA do not form helical shaped ParA structures in vivo but rather colocalize with the complete nucleoid. Polymerization and depolymerization is an profound mechanism to exert forces on relatively big objects such as plasmids and chromosomes. An important question is whether this is also the case in pB171 plasmid segregation. ParB colocalizes tightly with plasmids in pB171 and P1 and this appears to be the case as well for the ParB homologue TlpT in chemotaxis cluster positioning[17]. TlpT is a chemoreceptor bound to the cluster [18]. However in the minCDE system, MinE fulfilling a similar role as ParB, locates throughout the complete cell and as a consequence this generates spontaneous pattern formation by a Turing-like instability [5]. At least two diffusive components are needed for such a reaction diffusion mechanism.

It was shown by Ebersbach *et. al.* [15] that the *par2* plasmid partitioning mechanism generates an equidistant distribution of plasmids across the long axis of a rod shaped *E. coli* cell (see fig. 3). More recently it was established that retracting helical ParA structures are followed by plasmids suggesting that the ParA structure exerts a pulling force on plasmids [1] (also see fig. 1). Repetitively ParA structures spontaneously form and elongate until they encounter a plasmid, which initiates the ParA retraction. Mathematical modelling predicted that in order to obtain regular positioning by pulling filaments, the distance a plasmid is pulled should depend linearly on the initial length when a ParA filament first encounters the plasmid (length dependent pulling). This was verified experimentally (see fig. 2). In a proposed model the rate of plasmid detachment from a ParA filament was assumed to be somehow length dependent. It remained unclear what the molecular details could be that generated such a rule. In this thesis we extend that pulling model by including rapid ParB sliding along a ParA filament. We show that this automatically generates a length dependent detachment rate and as a consequence also length dependent pulling. However this model requires that the ParB copy number scales solely with the number of plasmids in a cell, and not with the cell volume. This prediction was tested experimentally by the group of Kenn Gerdes in Newcastle. It turned out that the

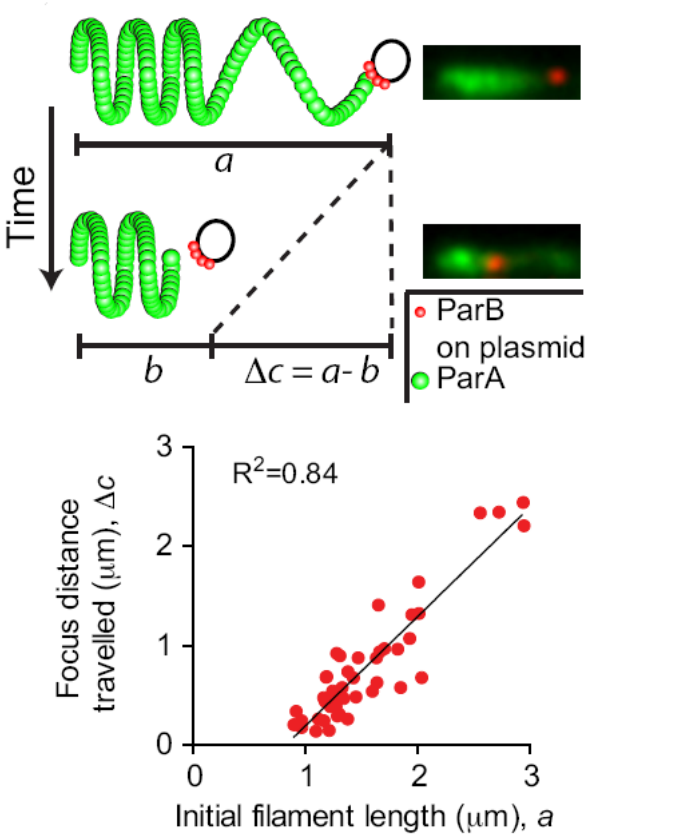

Figure 2: Above: cartoon visualizing the linear dependence of the distance a plasmid is pulled by a retracting ParA structure. Below:scatter plot of the length of ParA filaments versus the distance a plasmid is displaced under the influence of ParA [1].

ParB concentration was fixed and independent of plasmid copy number. With this knowledge the model was unable to generate proper plasmid segregation.

Vecchiarelli *et. al.* proposed that the ParA structure is not a ParA polymer but rather a gradient of ParA dimers as the P1 system doesn't exhibit a filament. They suggested that the plasmid with attached ParB stimulating the ATPase of ParA could dynamically influence the ParA distribution along the nucleoid. As a consequence plasmid could segregate as their movement is biased towards high ParA concentrations. We developed a theory that confirmed this idea and

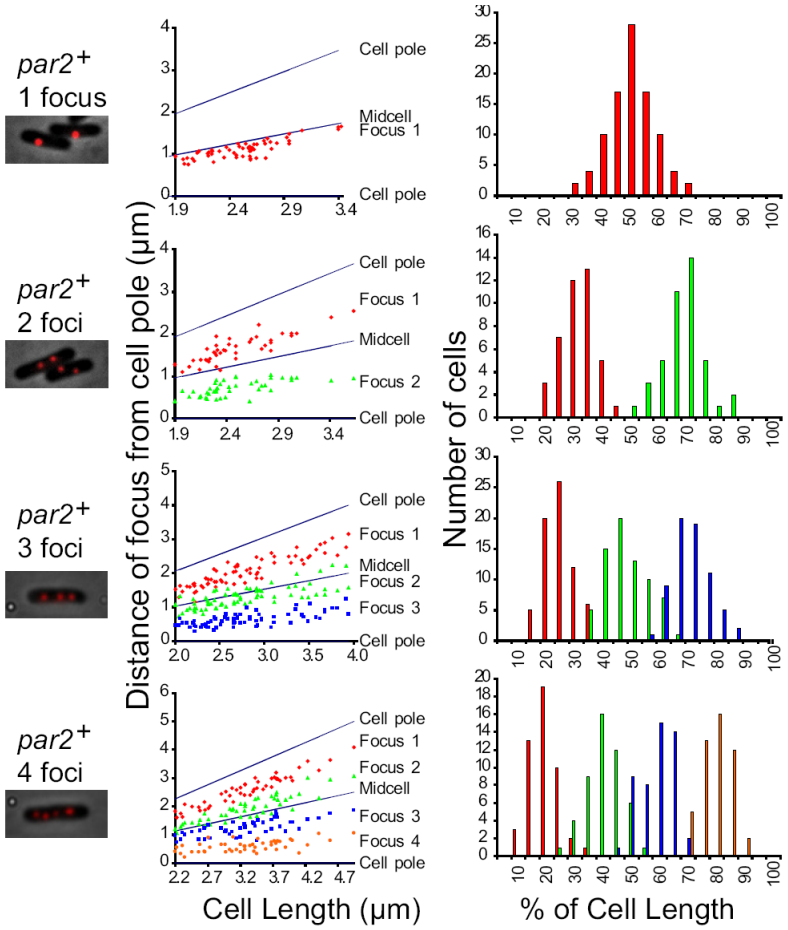

Figure 3: Histograms showing the distribution of plasmids along the long axis of *E. coli* cells. One plasmid locates primarily in the middle of the cell and in the case of multiple plasmids, they are partitioned equidistantly [1][15].

performed simulations to verify that in principle such a mechanism could lead to equidistant positioning. However it requires a very mobile plasmid, which is not observed experimentally [19] and taking into account the embedding of the linear structure into the two dimensional nucleoid surface, leads to the problem that the plasmid would diffuse away from the linear structure too frequently. Another argument against this model is the experimental observation that ParA can extend outside the nucleoid and induce plasmid motion in the cytoplasm (*personal comment* F. Szardenings). A biased diffusion mechanism however requires the nucleoid to act as a scaffold, so it would be difficult to explain these

observations with such a model. Considering the drawbacks altogether we do not favor this mechanism.

Following the idea that a gradient dynamically generated by the plasmid could generate plasmid segregation, we envisioned that small oligomers might diffuse along the nucleoid and upon encounter with a plasmid start to depolymerize and pull a plasmid. Again simulations lead to equidistant positioning though after careful inspection of the underlying physics we conclude that this mechanism is not physically feasible, because high diffusion by ParA oligomers would suggest a low drag coefficient by the Einstein relation. However a high drag coefficient is needed to be able to pull a relatively massive object such as a plasmid. As noted above in the biased diffusion model here ParA oligomers need the nucleoid as a matrix to exert forces, while experimental observations (*personal comment* F. Szardenings) suggest this is not strictly necessary.

As drag appears to be important for motility in a crowded, viscous medium such as the bacterial cytoplasm, we investigated the influence of drag on both a plasmid and a ParA polymer by solving the equations of motion (e.o.m.) for the plasmid as it is being pulled steadily by a ParA polymer. From this we can verify that this process induces length dependent pulling under certain conditions as experimentally shown in [1]. However with the assumption that only one polymer attaches to the plasmid and pulls it, it requires strong assumptions to achieve equidistant positioning. A genuine "tug of war" scenario where two filaments simultaneously connect and depolymerize in opposite directions is also unlikely to be the sole mechanism for equidistant positioning.

Lastly we worked out the idea that not ParB but ParA subunits or oligomers could bind to a ParA filament and slide along it to find the ends of the filament rapidly. Therefore the growth of filaments would be length dependent. In combination with a polymer pulling mechanism this could generate plasmid partitioning. If ParA binds tightly to DNA ParA oligomers of sizes on the order of $100nm$ could generate enough force to pull a plasmid significant distances, because the effect of an oligomer being reeled in towards the plasmid rather

than pulling it becomes negligible. In that case multiple oligomers that pull plasmids short distances, could induce equidistant positioning. The difference with the diffusing oligomers is that now they slide rapidly along ParA, but this is only transiently until they encounter DNA and can bind there tightly. The length dependency is then created because of the diffusive flux of ParAs generated by the sliding along the filaments. However the argument that ParA can extend off the nucleoid and reel a plasmid from the cytoplasm renders this idea unlikely as well. So both sliding of ParA subunit and polymerization of ParA are necessary requirements. If ParA binds weakly to DNA, the influence of drag could enhance further positioning, but it is not required and certainly not sufficient. We propose that a mechanism in which ParA polymers pull repetitively on plasmids that detach with a high rate could generate dynamic equidistant positioning of plasmids along the long cell of the axis. The length dependent positioning is due to ParA subunits sliding along ParA polymers that generate a length dependent growth rate of the filaments.

2 Results - Theory

2.1 ParA filament pulling model with influence of drag

2.1.1 One ParA filament, one plasmid

As experiments demonstrate that long linear structures pull on plasmids, the simplest explanation would be that ParA polymers retract and pull a plasmid along. Mathematical modelling indicated that with the assumption that a ParA polymer binds tightly to the nucleoid, and secondly that the plasmid has a certain constant probability over time of detaching from the filament, plasmids cannot be positioned equidistantly inside a cell [1]. However experimentally if one plasmid is present in a bacterium, it can oscillate along the long axis of a cell, but on average locates primarily in the middle of a cell. Regular positioning requires that filaments pull plasmids a distance that scales linearly with length of a ParA filament when it first encounters the plasmid (length dependent pulling, see fig. 2). However length dependent pulling could also simply be a consequence of Newton's third law. As filaments depolymerize, their viscous

drag reduces and therefore they induce less motion to a plasmid. In effect the plasmid is being pulled a distance that scales linearly with the initial length of the ParA filament at the moment of attachment. We investigated whether this mechanism could generate equidistant positioning.

The question we want to address first is whether a plasmid can be pulled to the middle of a cell and remain there by the pulling of a single filament. In addition we want equidistant positioning in the case of multiple plasmids. In general if a mechanism can meet these two requirements for varying cell sizes, we denote that this mechanism exhibits "length control". We start with the simple case of one plasmid in a cell of length L varying from $L_{min} = 2\mu m$ to $L_{max} = 3.5\mu m$ [1]. The aim is to position the plasmid at mid cell. It is intuitively clear that the length of the polymer l_0 and x_p the initial position of the plasmid can vary. So there is no way to "sense" the middle without further assumptions. A simple assumption to address this would be to argue that the ParA polymer extends to its nearest pole. So we take that the filament extends to the +pole. We assume that at the point of connection ParB depolymerizes ParAs with a constant rate. For simplicity we initially assume the plasmid does not detach from the filament. We model the hydrolysation by the plasmid and disconnection of ParA subunits from the polymer with an effective rate k_d. On the other tip end of the ParA polymer it can polymerize with a rate k_p.

We can envision two possible scenarios: one in which the filament size could decrease to zero before the plasmid reaches the +poles if $k_p < k_d$. In the other scenario $k_p \geq k_d$ so that the filament remains connected to the +pole all the time.

We proceed by looking at the first case. The index p denotes the plasmid, A the ParA filament. ζ_p is the drag coefficient of the plasmid, assumed to be time independent. ζ_A is the drag coefficient of the ParA filament bundle and $\vec{v_i}$ the velocity of either component along the long axis of a cell which we denote as the x direction. The equation of motion (e.o.m.) comes from Newton's third

law in a viscous medium:

$$\zeta_p \vec{v}_p = -\zeta_A \vec{v}_A$$

We assume that the drag coefficient of the filament is proportional to the number of subunits in it. We don't take into account that the number of subunits is an integer, but rather assume a continuous growth and detachment of the filament:

$$\zeta_A = \zeta_0 \left(\frac{n l_0}{a} - (k_d - k_p) t \right).$$

a is the size of a ParA subunit, n is the number of ParA filaments that a ParA filament bundle consists of. ζ_0 is the drag coefficient of one ParA subunit. The motion of the components is induced by a bundle of ParA filaments depolymerizing at the point of connection between plasmid and filament (from now on unless stated otherwise when we refer to the filament we mean the filament bundle). For a detailed derivation of the current section we refer to the methods section in appendix A.1. Taking into account that the velocities of the two components are in opposite direction this results in the following e.o.m.:

$$v_p(t) = \frac{\zeta_A(t) \, \frac{a k_d}{n}}{\zeta_p + \zeta_A(t)}. \tag{1}$$

We look at the position of a plasmid in the limit of a completely depolymerized filament:

$$\lim_{t \nearrow \frac{n l_0}{a(k_d - k_p)}} x_p(t) = x_p(0) + l_0 \frac{k_d}{k_d - k_p} - \frac{\frac{\zeta_p}{\zeta_0} a k_d}{n (k_d - k_p)} \ln \left[\frac{\zeta_p + \frac{\zeta_0 n l_0}{a}}{\zeta_p} \right].$$

Here we see that the initial position and the initial filament length cannot be eliminated in favor of L, so that exact length dependent pulling will not be possible. However if the plasmid drag coefficient is about the same as the initial length of the ParA filament: $\zeta_p \approx \zeta_0 n l_0 / a$, the distance that the plasmid is displaced does scale linearly with the initial length l_0 (see appendix A.1). The fact that l_0 can vary, does not influence the results considerably as long as it remains on the same order as ζ_p. In section 3.1 we report on deterministic simulations that indicate that positioning of one plasmid in the middle of a cell can be achieved. However we also need equidistant positioning of multiple plasmids. In the case of two plasmids, instead of equidistant positioning, the drag of the polymers is not high enough in order for them to segregate the plasmids as they will only pull them to mid cell, not to 1/4 and 3/4. This indicates that

this mechanism is not able to segregate plasmids. The drag coefficient of the ParA would have to change spontaneously as the plasmid number increase. An increase in ParA numbers due to new production by the newly created plasmid might be responsible for this.

The second possibility in which the ParA filament remains extended to the cell pole due rapid polymerization ($k_p \geq k_d$) can be discarded by the following consideration. The only way to position plasmids at mid cell would work, is if initial pulling would be quick but then slows down considerably in the middle of a cell because shorter filaments would not be able to induce enough motion of the plasmid. This generates effectively positioning in the middle. But this argument cannot hold because if a plasmid is effectively pulled to the middle in a big cell of $L_{max} = 3.5\mu m$ due to a considerable decrease in velocity around $\frac{1}{2}L_{max}$, it will surely not pull it to the middle of a small cell of length $L_{min} = 2\mu m$ in a timely fashion because a filament of length $l_0 = \frac{1}{2}L_{max} = \frac{7}{8}L_{min}$ cannot induce enough velocity to a plasmid. In the appendix A.1 this argument is made precise.

We stated at the beginning of this section that we assumed the plasmid never detaches. In the case of $k_p \geq k_d$ rapid plasmid detachment does not influence the result obtained above when a plasmid can reattach after a time period τ, since the polymer just remains attached to the cell pole in that time, so the length of the filament does not change. As a consequence even when a plasmid often detaches, the intuitive argument stated above is still valid. This is not necessarily true for premature detachment when $k_p < k_d$ because in time period τ, the filament can grow again as it is not necessarily elongated completely to a cell pole anymore.

The discussion in the previous paragraph brings us to another requirement of a polymer pulling model: the connection between ParA filament and plasmid through the ParA-ParB interaction cannot be too stable. If the interactions would be stable enough, two plasmids that are simultaneously attached to a filament (one at each tip end) would induce complete depolymerization of the ParA filament before detaching. Due to symmetry arguments, the plasmids

would meet each other halfway. This induces oscillations rather than equidistant positioning as can be seen in section 3.1. As a conclusion one polymer that depolymerizes with a rate $k_p < k_d$ and thereby pulls on a plasmid, combined with the assumption that the DNA has a high detachment rate, cannot be excluded on theoretical grounds only.

2.1.2 Two filaments, one plasmid

We proceed by investigating two opposing ParA filaments that can pull plasmids to induce positioning. Similar to the case of one filament there can be variation in initial position of the plasmid, so we assume that both filaments extend to their respective pole. It is unfeasible that only one of the filaments will stretch out to a pole because the microscopic details of filament growth at the tip are presumably the same for every growing filament in a cell. So if one filament stretches to the nearest cell pole we must have that $k_p > k_d$, so this will induce elongation of every filament given that cytoplasmic ParA subunits are ubiquitous and uniformly distributed. The following arguments are mathematically verified in appendix A.2.

Because of the argument made at the end of the previous section we have to assume that somehow the plasmid disconnects very often from the filaments. To analyze this idea further we assume that the time τ that the plasmid is connected to a filament is so short that the length of the filament does not change considerably: $l(\tau) \approx l_0$. For $k_d = 4s^{-1}$ this would on the order of seconds for filaments of typical lengths of a micron. This is not a unreasonable assumption.

If drag would act as the major contributor to length control, this mechanism should be able to cope with several situations. Experiments point out there are two important ones that differ significantly. In the first scenario we have two filaments that extend to either pole pulling on a plasmid in opposing directions, the effective velocity with which the plasmid moves is now the difference of both pulling on it separately. In this limit of short attachment times it is unlikely that both filaments attach to it simultaneously, so that this statement is justified. W.l.o.g. $x_p \leq \frac{1}{2}L$ so by eq. 17 for two opposing filaments (+ and −) the speed

of the plasmid is:

$$v_p(t) = \frac{k_d\,(L - x_p)}{\frac{\zeta_p}{\zeta_0} + \frac{(L-x_p)n_+}{a}} - \frac{k_d x_p}{\frac{\zeta_p}{\zeta_0} + \frac{x_p n_-}{a}}. \tag{2}$$

As we think it is unlikely that the number of filaments inside a bundle can differ significantly, we assume $n_- = n_+ = n$. Of course we require timely positioning and this puts restrictions on the values ζ_p/ζ_0. We require that a plasmid that is near a cell pole, e.g. $x_p = 0.1L$, movement towards the middle needs to occur quite rapidly. This limits ζ_p/ζ_0 to $10^2 - 10^3$ for relevant values ranging from L_{min} to L_{max} and $k_d = 4s^{-1} - 40s^{-1}$ and $n = 1 - 10$. In table 1 the velocities and displacements are listed.

On the other hand sometimes, there is only one polymer present that pulls on the plasmid. In that case we can simply use eq. 17 again for the velocity of the plasmid. Since experimentally no plasmids are observed further than $0.2L$ away from mid cell, that polymer should not have the power to pull a plasmid further away from the centre. But for the relevant regime of $\zeta_p/\zeta_0 = 10^2 - 10^3$, the velocity only differs a factor of 1.8 at most from the velocity calculated in eq. 2, this induces significant erroneous motion towards the cell pole.

We conclude that it is unlikely that a plasmid rapidly switches connections between two opposing filaments without further assumptions. In the case that the ParA subunit copy number inside a cell scales with plasmid copy number and not with cell size, there are no theoretical objections against the proposition that filament drag could be the main reason for equidistant positioning. Whether this assumption is realistic remains to be seen.

2.2 ParA filament pulling model with ParB levels determining the detachment rate

In the previous section we concluded that a connection between a ParA filament and the plasmid that is very stable leads to oscillations rather than equidistant positioning. The number of ParB subunits bound to the plasmid influences the strength of the interaction: more binding sites filled with ParBs strengthen the link between plasmid and filament. We investigated the idea that the number of

ParB subunits determines the rate of detachment from a pulling ParA polymer and thereby induce equidistant positioning. *parC1* and *parC2* have respectively 17 and 18 ParB subunit binding sites [10] [11]. We expect that al these binding sites are occupied most of the time and that they are all involved with binding ParA subunits along the side of the filament end. It has been reported that ParB can form high molecular weight nucleoprotein complexes in combination with the centromere binding locus [10] [11] [20]. This suggests that the number of ParB subunits that colocalize with the plasmid is not limited to 35, which gives rise to a possibility of varying ParB levels at the plasmids.

It has been reported that the length a ParA filament pulls a plasmid is linearly dependent on the length at the moment that the filament and plasmid initially connect [1] (see fig. 2). We built a model in which the cytoplasmic ParB subunits can bind to a ParA filament and diffuse in a linear fashion along it. When a plasmid is attached to an end of a ParA filament, it is assumed that the ParB unit will bind to the plasmid, as ParB has an affinity for the specific *parC* locus. As ParB also has affinity for ParA the link between filament and plasmid will strengthen. Since it is more likely that a ParB unit attaches to a longer filament compared to a short one, the number of ParB units that are absorbed by a plasmid will also be higher for the longer one. This is under the assumption that linear diffusion and absorption are rapid compared to the time it takes a ParB unit to unbind from a filament before it reaches a plasmid and binds to it. The idea is reminiscent of the mechanism that generates a length dependent depolymerization rate of microtubules [21].

We model the nucleoid as one dimensional along the long axis of size L in a rod shaped bacterial cell. Let $[B]$ be the cytoplasmic concentration of ParB subunits (unit: m^{-1}), k_{on} the binding rate of ParB binding to a ParA filament and k_{off} the unbinding rate from a plasmid. The differential equation for B_p, the number of ParB units bound to a plasmid that is connected to a ParA filament of length $l(t)$ at time t is given by the following differential equation:

$$\partial_t B_p = k_{on}\,[\mathrm{B}]\,l(t) - k_{off} B_p \ .$$

As noted previously this is under the assumption that all ParB units that bind to the filament are absorbed instantaneously by the plasmid (i.e. rapid diffusion along the filament with negligible unbinding) and furthermore the amount of cytoplasmic ParB units binding to the plasmid directly is negligible compared to the amount that comes from the filaments. These assumptions can be realistic as there is experimental evidence of rapid linear diffusion of proteins sliding along DNA of lengths of multiple microns before unbinding with a diffusion constant as high as $0.6\mu m^2/s^{-1}$ [22]. Lastly another assumption is that the cytoplasmic ParB concentration is unaffected by the number of ParB at the plasmid. Since the copy number of ParBs in a typical *E. coli* bacterium lies in the order of thousands, this requirement can easily be met. Since the process of ParB binding and diffusion relaxes rapidly compared to changes in the lengths of the ParA filament we can assume a steady state situation so that the ParB levels at the plasmid will be:

$$B_p = \frac{k_{on}}{k_{off}} [\mathrm{B}]\, l(t). \tag{3}$$

This means that B_p is proportional to $l(t)$. In order to obtain length control we have to set conditions on the cytoplasmic ParB concentration. The *parA* and *parB* genes lie on the plasmids themselves. If we assume that every plasmid creates a fixed number B_0 of ParB molecules we obtain:

$$[\mathrm{B}] = \frac{n_p B_0}{L}\ . \tag{4}$$

To obtain length control the plasmid needs to detach from a filament at the right moment. So we introduce a threshold value T for B_p below which the plasmid is not sticky enough anymore to be pulled along. The drag due to the size of the plasmid inside a viscous medium as the cytoplasm of a bacterium could induce such a detachment, though we also require $\zeta_p \ll \zeta_0 \frac{l(t)}{a}$ to ensure that the ParA filament is not reeled in. For instance when the ParA filament is tightly bound to the nucleoid we can meet these requirements. If the parameters k_{on} and k_{off} are as follows:

$$\mathrm{T} = \frac{k_{on} B_0}{2k_{off}}\ , \tag{5}$$

we obtain by eqs. 3 and 4 that $B_p = \mathrm{T}$ at a ParA filament length of

$$l(t) = \frac{L}{2n_p}\ .$$

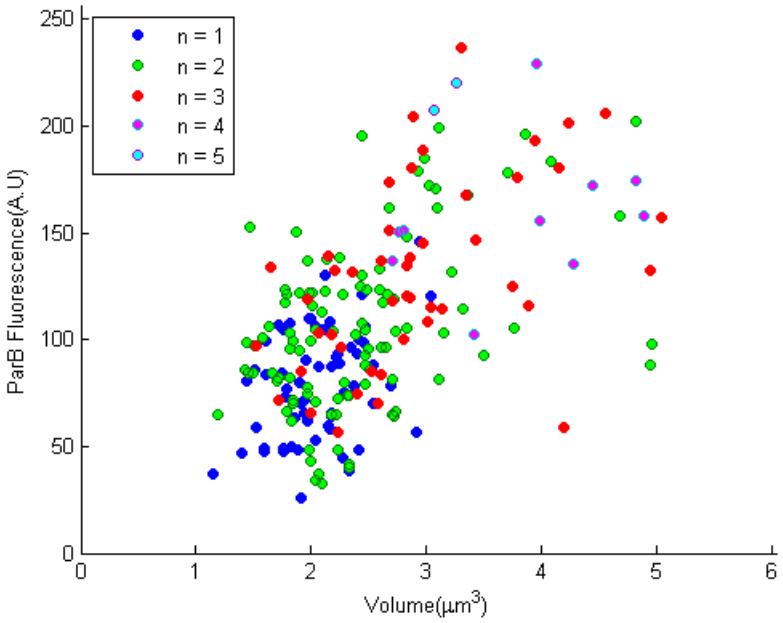

Figure 4: Data from the group of Kenn Gerdes (unpublished). Scatter plot of the light intensity due to ParB-GFP expression in a single cell versus the volume of the cell. Since ParB binds to pB171 plasmids, n, the number of foci visible in the confocal images of ParB-GFP, should reflect the number of plasmids in a cell. The fluorescence intensity seems to scale with the volume of the cell rather than with the number of foci. Data was analyzed with Microbe Tracker, a MATLAB plugin developed by Jacobs-Wagner *et. al.* . Z-stacks of confocal images with the ParB-GFP signal were obtained and summed over which results in the total fluorescence in a plane. In addition with phase contrast images, the outline of cells were obtained which were used to identify the intensity signal from within a cell and the volume. The background intensity was subtracted and the number of cells that were analyzed is 242. The number of bright foci was determined with spotFinder which is part of the Microbe Tracker plugin.

In effect the plasmid will detach on average from that filament at this length, so that we obtain regular positioning for plasmids provided that filaments elongate until they encounter a cell pole or a plasmid. In the case of two plasmids attached to one filament, the flux of ParB reaching each plasmid will be on aver-

age half compared to the case where only one plasmid is attached to a filament. This results in detachment at lengths of $\frac{L}{n_p}$. In effect this should be the spacing between plasmids which is equidistant. Stochastic simulations explained in section 3.2 verified that this mechanism can meet the experimental distributions of plasmid positions for different cell sizes and different plasmid copy numbers. The big assumption of this mechanism is eq. 4. Experiments indicated that the ParB concentration is constant rather than varying with cell size and plasmid copy number (see fig. 4).

As a consequence of eq. 3, i.e. a constant density of ParB, and the assumption that the threshold value is a constant T, the filaments will pull the plasmid until the length of the filament is equal to

$$l(t) = \frac{k_{off}\mathrm{T}}{k_{on}\,[\mathrm{B}]}\ .$$

This means that filaments pull the plasmid until they are of a specific length irrespective of the cell length, thus the distance pulled does depend linearly on the initial filament length, as experiments suggested [1]. However the plasmid does not get positioned at the right place in a cell. We conclude that this mechanism is not used by *E. coli* to partition plasmids equidistantly.

2.3 Biased diffusion model

ParA polymerizes *in vitro* and forms linear structures on the nucleoid though it remains unclear if ParA actually polymerizes *in vivo* [13][15]. We investigated alternative models that do not incorporate ParA polymerization. The first one proposed by Vecchiarelli *et. al.* in [2] encapsulates the idea of the plasmid performing diffusive motion biased by the concentration of ParA subunits bound to the nucleoid locally at the plasmid. Cytoplasmic ATP bound ParAs are assumed to remain dimers and they can bind anywhere to a one dimensional structure on the nucleoid. The ParA subunits can diffuse on that structure with diffusion constant D_A. This linear structure could be due to the nucleoid itself or a sort of railway track present on the nucleoid surface. Exactly how bacterial chromosomes are organized remains elusive up to now. Berlatzky *et. al.* showed that in *Bacillus subtilis* the nucleoid organizes into a helical structure during

replication [23]. In *E. coli* the circular chromosome is thought to fold into a linear fiber during G1 phase (before initiation of chromosome segregation)[24]. Another option explaining the reduction of dimension is that ParA subunits self assemble into a linear structure whilst maintaining diffusive motion inside it. We performed stochastic simulations to test this hypothesis of self organization and for further details we refer to sections 2.5 and 3.5.

Other assumptions of the model are as follows: ParA-ATP can hydrolyze ATP spontaneously with a low rate k_A and with a high rate $k_{AB} > k_A$ in the presence of ParB which itself is active only at the plasmid. Note that the stimulated ATP turnover is a second order reaction, so k_{AB} has units $s^{-1}\#molecules^{-1}\ length$, but by multiplying with the concentration of plasmids $\frac{\#Plasmids(site)}{\mathrm{d}x}$ at a site of length dx at the grid, we can compare it with k_A which is a first order rate constant. Therefore from here onwards when we refer to "k_{AB} in the presence of one plasmid" to compare it to k_A, we actually compare $k_{AB}\frac{1}{\mathrm{d}x}$ with k_A.

The plasmid can also diffuse with a diffusion constant D_p on the line, but this diffusion constant is dependent on the local ParA concentration: in the absence of ParA the plasmid diffuses with $D_p > D_A$. We need this to ensure that the ParA distribution appears static from a the perspective of a freely diffusing plasmid. But in addition we assume this diffusion constant decreases to zero in the presence of multiple ParA subunits that anchor the plasmid to the nucleoid.

We expect that the increased unbinding rate of ParA at the location of the plasmid x_p induces a local minimum in the ParA concentration, because locally at the plasmid ParB stimulates the ParA ATPase activity. Since the ADP bound form of ParA does not bind to DNA, after hydrolysation ParA will unbind from the nucleoid. Subsequently the subunit remains in the ADP bound form and after a "waiting time" that is long compared to the diffusive motion of all components in the system, it is converted into an ATP bound form again that is potent to bind the nucleoid with a high affinity. This waiting time reflects the experimental evidence described in [2] that reports on the low conversion rate from an ADP to ATP bound ParA protein. This ensures that the cytoplas-

mic concentration of cytoplasmic ParA-ATP molecules is uniform in the cell. As a consequence we can view J, the flux of ParAs binding to the nucleoid as independent of position along the chromosome. To perform an analysis of the concentration profile of ParAs we look at the nucleoid as the interval $[0, L]$. We denote with $A(x)$ the concentration of nucleoid bound ParAs at position $x \in [0, L]$. As the ParAs cannot escape from the nucleoid without unbinding we demand zero flux boundary conditions at the cell pole: $\partial_x A(0) = 0 = \partial_x A(L)$. Furthermore we neglect the spontaneous hydrolysation because this does not contribute to accurate positioning of a plasmid. Experimentally the rate of spontaneous hydrolysation is on the order of $4 \cdot 10^{-4} s^{-1}$ [2] which is a lot lower than typical rates of $5s^{-1}$ that we used for k_{AB} in the presence of one plasmid in our stochastic simulations. Since the ParAs diffuse on the nucleoid this results in the following boundary value problem:

$$\begin{aligned} &\partial_t A(x,t) = D_A \partial_x^2 A(x,t) - k_{AB} A(x,t) \delta(x - x_p) + J(t) \\ &\partial_x A(0,t) = 0 = \partial_x A(L,t) \ \forall t \geq 0 \end{aligned} \tag{6}$$

Now we assume that the system reaches its steady state, so that $J \neq J(t)$ and $\partial_t A(x,t) = 0$. This approximation is only valid if the effective diffusive motion of the plasmid is slower than that of the individual ParA subunits bound to the nucleoid. But as the diffusion constant of the plasmid is slowed down to zero as $A(x_p)$ increases this assumption is reasonable.

We are interested in the force that drives the motion of the plasmid. The dynamics are governed by the flux of ParAs coming in from either side of the plasmid. When one plasmid is located at $x_p < \frac{L}{2}$, more ParA units will diffuse towards the plasmid from the +side ($x > x_p$) than the −side. Since the diffusion of the plasmid is biased towards high $A(x)$, it will move effectively in the + direction. We can quantify this by determining the flux $\mathcal{F}_\pm(x_p)$ of ParAs coming in from the ± direction. We use Fick's law to determine the flux from the gradient of $A(x)$:

$$\begin{aligned} \mathcal{F}_-(x_p) &= -D_A \partial_x A(x_p^-) = -D_A \lim_{\epsilon \to 0} \int_0^{x_p - \epsilon} \mathrm{d}x \ \partial_x^2 A(x_p) = J x_p \\ \mathcal{F}_+(x_p) &= -D_A \partial_x (x_p^+) = +D_A \lim_{\epsilon \to 0} \int_{x_p + \epsilon}^{L} \mathrm{d}x \ \partial_x^2 A(x_p) = J(L - x_p) \end{aligned} \tag{7}$$

If w.l.o.g. it is assumed that $x_p < \frac{L}{2}$, then $\mathcal{F}_+(x_p) > \mathcal{F}_-(x_p)$, only at $x_p = \frac{L}{2}$ they balance and no net direction is preferred. A similar analysis can be performed for multiple plasmids which is shown in section 2.6. We conclude that this mechanism generates length control. In section 3.3 we explain the details of stochastic simulations that were performed to verify that this mechanism could provide accurate plasmid positioning and segregation.

The major difficulty with this mechanism is the assumption that the plasmid diffuses only along the one dimensional linear structure. In reality it is embedded in the bacteria and since we require $D_p > D_A > 0$ the plasmid is very likely to diffuse away from this structure every time it makes a diffusive movement. The fact that it is immobilized by ParA most of the time does not help since it has to diffuse along the linear structure too in order to get the right positioning. We cannot arbitrarily lower D_p to prevent escape, because then rate of movement along the linear structure will decrease accordingly so that eventually it takes the plasmid longer than a complete cell cycle to move to the middle of a cell. It is reported in [19] that in *E.coli* a test plasmid of similar size as pB171 without the par operon diffuses with a constant of $D_p = 5 \cdot 10^{-5} \mu m^2/s$ and that its diffusive motion is confined to a region of $0.28 \mu m$. This diffusion constant is too low to get timely positioning and the confinement would argue against biased diffusion as the driving force of motion as well. Simulations of a one dimensional ParA distribution embedded in a 2D nucleoid surface suggest that for a diffusion constant $D_p = 0.1 \mu m^2/s$, a rather high value necessary to obtain accurate positioning in a purely 1D model, escape from the line is highly detrimental for plasmid positioning as the plasmid explores the complete 2D surface before returning to the ParAs. Lastly recent experiments suggest that in filamentous cells ParA is able to extend outside the nucleoid region into the cytoplasm and "grab" a plasmid to pull it back to the nucleoid. In a biased diffusion mechanism this would not be possible as the nucleoid acts as a scaffold for the ParA molecules to immobilize the plasmid. In absence of such a matrix ParA cannot direct the motion of the plasmid. Therefore we conclude that this mechanism is not the one used by bacteria to position plasmids.

2.4 ParA oligomer pulling model

As the biased diffusion model could naturally generate length control, it is expected that some form of diffusion along the long axis of the cell might be important in the pB171 plasmid partitioning system. Diffusion has the intrinsic feature that it could "sense" the cell size and inter plasmids distance when they influence the ParA distribution. Trying to find a model that combines this relevant feature with the attractiveness of polymers as they could exert forces on a plasmid, we investigated the idea that ParA subunits might pull the plasmid in a similar way as the model in which filaments pull with drag included, but instead of forming static long polymers, ParA subunits might form oligomers that diffuse along a linear one dimensional structure. This pulling requires an attractive short range interaction between the ParA and ParB subunits. We suggest this could be a Van der Waals force or an electrostatic force. Sugawara *et. al.* suggest that a gradient of diffusible molecules can exert a force on a macroscopic element based on thermodynamic arguments in [25]. Implicitly they assume an attractive interaction potential as the diffusible particles favor adsorption to the macroscopic element on a series of binding sites.

In the following section we assume that ParA oligomers diffuse in the same manner as section 2.3. At the location of a plasmid, we propose that the plasmid can be pulled along by ParA oligomers locally around the plasmid with rate k_{AB}. This rate encompasses both hydrolysation and depolymerization of the oligomers. As the oligomers are hydrolyzed they unbind from the nucleoid. This creates again a gradient of the ParA distribution but bear in mind that this is a gradient of oligomers, rather than ParA subunits. The ParA distribution of oligomers is again governed by eq. 6. So the effective mechanism that induces motion of the plasmid is again the difference in flux of ParAs that reach the plasmid as pointed out in eq. 7.

In the previous section we needed a high plasmid diffusion constant D_p, but in this mechanism the plasmid diffusion is only a source of noise. This mechanism works best if the plasmid does not diffuse at all, though a large drag coefficient ζ_p would be dramatic because oligomers would get reeled in rather

than pulling a plasmid along. The question remains whether there is enough middle ground to allow positioning of plasmids.

In section 2.1.1 we discussed the influence of drag on the movement of a ParA filament pulling a plasmid. In eq. 14 we saw that in the limit that a plasmid has far more drag than a ParA subunit, $\zeta_p > \zeta_0 \nearrow \infty$, the plasmid remains stationary and the ParA filament is reeled in by the plasmid. To make an estimate for ζ_p, we use the Einstein relation:

$$\zeta D = k_B T \ . \tag{8}$$

Although the estimate from [19] is $D_p = 5 \cdot 10^{-5} \mu m^2/s$ is very low (a typical timescale to diffuse a distance of $100nm$ which is comparable to the size of the plasmid, would be $200s$), we will assume a higher diffusion constant of $D_p = 10^{-3} \mu m^2/s$. Estimates for diffusion constants of mRNAs and GFP proteins are respectively $10^{-3} - 10^{-2} \mu m^2/s$ [26] and $8 \mu m^2/s$ [14]. By eq. 8 we obtain an estimate: $\zeta_p \approx 4 \cdot 10^{-6} kg/s$.

To test whether this mechanism could generate equidistant positioning, we performed stochastic simulations in which D_p was initially set to zero and ParA oligomers diffuse with D_A. Lastly with rate k_{AB} the oligomer depolymerizes completely and in effect the plasmid is moved the size of this oligomer. This model worked with a variety of sizes for the oligomers, though for a size of $50nm$, which we estimate as 20 ParA subunits, the positioning is not accurate enough anymore compared to the experimental results. In addition we note that accuracy of positioning increases as the oligomer size decreases. Furthermore reeling in of the oligomer is not taken into account, though the mechanism works for values of $D_A = 10^{-3} - 10^{-1} \mu m^2/s$. This means that even though reeling in could occur, with our estimate $\zeta_p \approx 4 \cdot 10^{-6} kg/s$ the limit of $\zeta_p/\zeta_0 \nearrow \infty$ certainly does not apply. So as eq. 15 reveals, the plasmid will move even though the oligomers could be reeled in too. For a typical oligomer size of $100nm$ [16] that diffuses with the relevant rate of: $D_A = 10^{-3} \mu m^2/s$, the plasmid will displace a distance of $5nm$ if we assume $D_p = 10^{-2} \mu m^2/s$. In the simulations accurate positioning by pulling these distances could be achieved, given that there is no plasmid diffusion. Premature unbinding seems like a source of noise. If it occurs

only in a moderate fraction of the occasions, this might not be disastrous for the mechanism as it relies on numerous pulling events by different oligomers. It is the combined action that induces plasmid motion.

The attractive force between ParA and ParB subunits that is required, could solve the problem of a plasmid diffusing away from the one dimensional linear structure. Further details on stochastic simulations in which we allowed for plasmid diffusion, we refer to section 3.4. The basic result is that for a plasmid diffusion constant of $D_p = 10^{-2}\mu m^2/s$ which was needed above to ensure enough plasmid displacement, the randomization of the plasmid position due to diffusion away from the ParA filaments is too severe to obtain equidistant positioning. Therefore this model encountered eventually the same problem as the biased diffusion model did.

2.5 Linear self organization of ParA

In the previous section we arrived at the conclusion that diffusing oligomers had the problem that they were not able to induce significant motion of plasmids. Apart from this, recent experimental results also suggest that ParA can extend transiently outside the nucleoid region into the cytoplasm to recruit cytoplasmic plasmids (*personal comment* F. Szardenings). Since the oligomers need the nucleoid DNA to act as a scaffold, it seemed unlikely that pulling oligomers could explain these findings.

Here we investigate whether self organization of diffusing oligomers into one filamentous structure could induce a more structure that has a high enough drag to induce plasmid motion effectively and stable enough to extend outside the nucleoid by interactions between oligomers that are in close proximity.

To see if self organization of oligomers into linear filaments is feasible, we simulated with a spatial Gillespie algorithm [27][28] the movement of oligomers on the surface of a cylinder that represents the nucleoid. This surface is divided into rectangular sites of size $\mathrm{d}x_{\parallel} = 100nm$ along the long axis of the cylinder and sizes of $\mathrm{d}x_{\perp} = 2.5 - 10nm$ along the circumference. Multiple oligomers

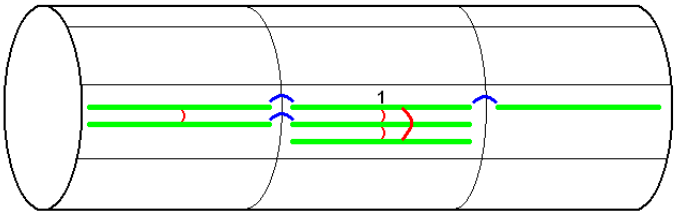

Figure 5: cylinder representing the nucleoid. The surface is divided into rectangles of size $\mathrm{d}x_{\parallel} = 100nm$, $\mathrm{d}x_{\perp} = 20nm$, not drawn to scale. ParA oligomers are shown in green, Head-Tail interactions (affinity H)between neighboring oligomers are shown in blue and lateral or "side" interactions (with affinity S) between oligomers at the sharing the same site with periodic boundary conditions are indicated in red. Oligomer 1 has an energy level of $-2H - 2S$.

can occupy a site. We postulate a "Head-Tail" affinity (H) between oligomers of neighboring sites along the long axis and a side affinity S between oligomers at the same site indicated in blue and red respectively in fig. 5. In absence of any oligomers at the same or neighboring sites, the oligomers are free to diffuse along the long axis with rate $\frac{D_A}{\mathrm{d}x_{\parallel}^2}$ and along the circumference with rate $\frac{D_A}{\mathrm{d}x_{\perp}^2}$. To describe the kinetics in the presence of interactions we refer to Arrhenius' rate law. The rates of the transitions between states A and B, with associated energy levels E_A and E_B respectively as shown in the energy landscape in fig. 6, is given by:

$$\begin{aligned} k_{A\to B} &= F \ \exp\left[\frac{E_A - E^{\ddagger}}{k_B T}\right] \\ k_{B\to A} &= F \ \exp\left[\frac{E_B - E^{\ddagger}}{k_B T}\right] \ . \end{aligned} \tag{9}$$

F is referred to as the attempt frequency and $E^{\ddagger}$ the activation energy level. W.l.o.g. we set the energy of a freely diffusing oligomer as 0. We assume that Head-Tail binding leads to a lower energy level of $-H < 0$ for both oligomers. Likewise lateral interactions lead to levels $-S < 0$ or $-2S$ depending on the number of oligomers at the same site with assumed periodic boundary conditions. In effect oligomer 1 in fig. 5 has an associated energy of $-2H-2S$ because it interacts with two neighboring filaments at the same site. Furthermore we propose that only one head can bind to a tail and due to lateral alignment those

interactions are limited to its nearest neighbors. In effect the energetically most favorable state has $E = -2H - 2S$. All interactions between oligomers are supposed to occur when possible.

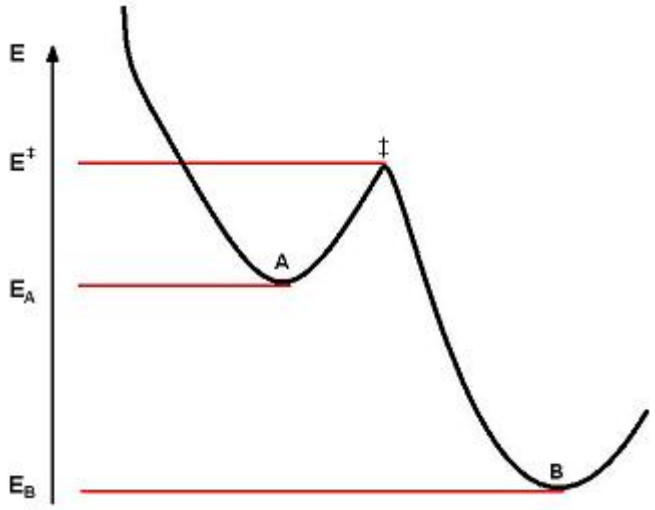

Figure 6: Energy landscape that illustrates Arrhenius' rate law. State A and B have energy levels E_A and E_B respectively. $E_A > E_B$, so state B is more stable. To go from A to B, the energy barrier $E^\ddagger - E_A$ has to be overcome, this is reflected in eq. 9.

If such an energy level E of an oligomer has $E < 0$, this oligomer must have associated bonds. In that case if the new site has no oligomers, all bonds have to be broken so $E^\ddagger = 0$, equal to the free diffusive energy level. On the other hand if the new site does have at least one oligomer, some lateral interaction remains during the movement so the energy barrier is lowered: $E^\ddagger = -S$. If no bonds existed (free diffusion), $E^\ddagger = 0$. The last thing we have to determine in eq. 9 is F. In the case of free diffusion, F is equal to the normal diffusion rate because $E = 0 = E^\ddagger$, but in principle this can change when bonds are involved. The rate now involves breaking bonds as well as diffusive motion to a neighboring site. Let f be the attempt frequency for breaking bonds. If we assume that both processes are necessary and occur consecutively we obtain the

following equation:

$$\frac{1}{F} = \frac{1}{f} + \frac{1}{k_d} \tag{10}$$

f is not known but from eq. 10 we infer that F is less or equal to the free diffusive rates. Simulations are done with the values $D_A = 5\mu m^2/s$, F equal to free diffusion rate, dependent whether the gridsize and the direction $\parallel$ and $\perp$, $H = 10k_BT$ and $S = 1.3k_BT$. For further details on the the results we refer to section 3.5. Details on the code can be found in appendix B.5.

2.6 ParA filament pulling model with ParA sliding

Varying the bond strengths in the model from the previous section results in the last mechanism we investigated. Rather than a couple of k_BT we now assume that the Head-Tail affinity is very strong, comparable to a covalent bond on the order of 10^2k_BT. Furthermore instead of a rather low affinity for DNA which was necessary to allow oligomer diffusion on the nucleoid we now assume tight binding, which renders ParA rather immobile on the nucleoid. By comparing the DNA binding and unbinding rate we can infer that B, the DNA binding affinity of P1 ParA lies around $B = 7k_BT$ [2]. If lastly we decrease the oligomer size to that of ParA subunits we have arrived at polymerization of ParA filaments. However with an extra feature: the ParA subunits can bind anywhere along the filament due a weak lateral interaction S. Thus this model contains aspects of both polymerization and diffusion.

By tuning the parameter values in the way described above we envision that ParA will polymerize, but the growth of polymers originates primarily through the actions of ParA subunits binding along the complete filament and sliding to the tips where they bind tightly. The binding along the length could be through a limited ParA-ParA affinity which is not unreasonable since they interact *in vivo* and *in vitro*. The interaction should not exceed tens of k_BT to allow for sliding, which is similar to the situation for ParB in section 2.2. However at the tip, the binding should be strong so that we obtain ParA polymers.

From the analysis on the effect of drag on plasmid motion induced by pulling polymers, we concluded that the rate of detachment is required to be high and

the efficiency of pulling would have to be low. Biologically this could be a relevant case if the plasmid detaches from the ParA polymer regularly due to loss of ParA-ParB interactions upon hydrolysation of ParA. A low efficiency can be realized if the depolymerization of one subunit does not induce plasmid displacement equal to the subunit size, but only a fraction on time average.

We consider the case of two filaments extending from the poles to one plasmid. Since ParAs can now slide to the ends of polymers and attach, the ParA polymerization rate is effectively dependent on the length of the filament. If the polymer grows and encounters a plasmid, the plasmid will acts as a sink for the ParA subunits that slide into that tip due to ATP hydrolysation. Since this sliding is itself linear diffusive motion we can apply eq. 7 for the distribution of sliding ParAs. The boundary conditions are correct as long as the filaments extend to their nearest cell poles. From section 2.3 we know that the force emerges from the flux difference of ParAs coming from either filament:

$$\mathcal{F}_+(x_p) - \mathcal{F}_-(x_p) = J\,(L - 2x_p)\,. \tag{11}$$

Now J the flux of binding ParAs to a filament depends on the length of the filaments and the density of active (ParA-ATP)$_2$ dimers. The difference with the ParB sliding scenario lies in the fact that it rather the *difference* of ParA coming in to the plasmid from the + and − side through two opposing ParA filaments rather than the *absolute* number of ParB sliding in from one filament being critical. To see this we note that on average one ParA subunit cycles constantly through the following stages: as an active cytoplasmic ParA-ATP it binds to the nucleoid with rate k_{on}, then it slides with diffusion constant D_A rapidly to the tip of the filament where it encounters the plasmid. There the plasmid binds to the ParA subunits with rate k_b and hydrolyzes it with rate k_{AB}. Then it becomes an inactive ADP bound form, and after the waiting time τ_{WT} it once again becomes an active cytoplasmic ParA subunit. Since the conversion step is rate limiting [2], this means that the waiting time is much longer than the typical times for all other stages in the process. Therefore we can approximate the flux J as the *density* of ParA subunits coming out of reservoir per waiting time. So the *number* of ParA subunits coming out of the reservoir in a waiting

time divided by the length of the cell is the flux:

$$J = \frac{A_0}{\tau_{\mathrm{WT}}\ L}.$$

A_0 is a proportionality constant which reflects the absolute ParA number that is turned over in one cycle ($\propto k_{AB}$). Inserting this in eq. 11 we see that by balancing τ_{WT} and k_{AB} the difference in fluxes coming in from the + and − sides can decrease to zero at $x_p = \frac{L}{2}$. This will be the distance between the plasmid and the nucleoid poles if one plasmid is present in the cell. Furthermore if two plasmids turnover ParAs at both tip ends of a filament, the flux of incoming ParA at one end of the filament is effectively halved, so that the inter plasmid distance becomes $\frac{L}{n_p}$. This means that this mechanism exhibits length control: it positions one plasmid in the middle and partitions multiple plasmids equidistantly. In section 2.6 we report on stochastic simulations that verify this theory.

In section 2.1.2 we carefully investigated that with a constant polymerization rate, length control was unlikely to be achieved even if the plasmid has a high detachment rate. The crucial difference why the mechanism of this section can in fact generate length control lies in the efficiency of pulling combined with the length dependent polymerization. A low efficiency ensures that it is primarily the influx of sliding ParAs rather than the ParA polymers itself that are being hydrolyzed. Furthermore the growth is dependent on the length so that in effect longer filaments reach out to connect to a plasmid more often and thereby pull on it more often. This is in contrast to eq. 2 which assumes that both filaments pull on it equally often, which lead to the problem that one filament could pull it to a cell pole. In this scenario short filaments cannot connect sustainedly enough to pull plasmids completely to a cell pole. This feature is verified in the simulations.

3 Results - Simulations

3.1 ParA filament pulling model with influence of drag

To see whether one ParA polymer pulling at a plasmid could position it at mid cell, we performed a deterministic simulation in MATLAB in which one polymer alternately extending from either + or −pole would attach to a plasmid and pull it to the position determined by eq. 15. The position of the plasmid over time resulting from in total 100 pulling events is shown in fig. 7. To obtain this result we used $\zeta_p/\zeta_0 = 5 \cdot 10^3$ and we assumed that there is no time in between consecutive pulling events. Varying L the cell length does not considerably change the results shown in fig. 7. We have set $n = 1$,the length of the cell $L = L_{min}$, the polymerization rate $k_p = 0$ and the ParA subunit size $a = 2.5nm$.

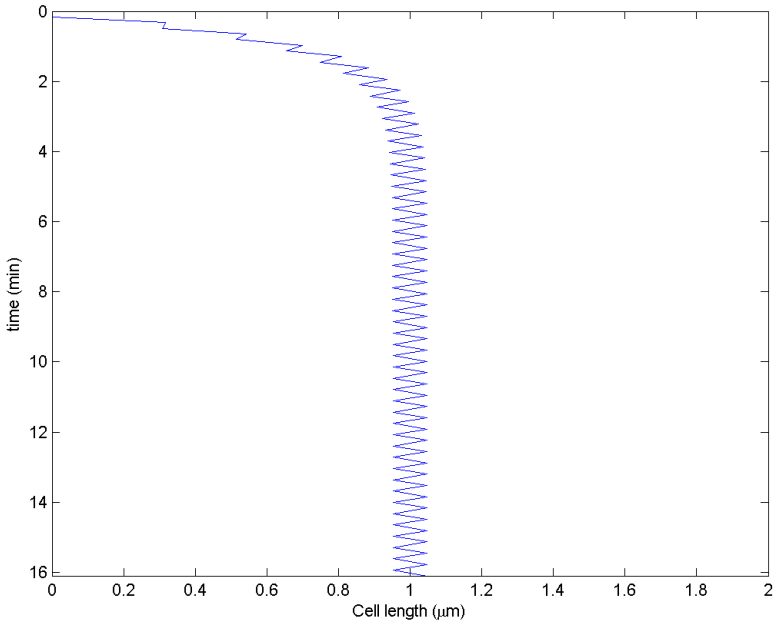

Figure 7: Plasmid trajectory plot over time, with multiple complete depolymerization events of ParA filament that alternately extend from the + or −pole initially. The initial position is the −pole to show that timely positioning at mid cell is possible. Parameter values are: $\zeta_p/\zeta_0 = 2 \cdot 10^3$, $n = 1$,$L = L_{min}$ $a = 2.5nm$ and $k_p = 0$.

Strictly speaking the plasmid performs oscillations around mid cell, but this might not be distinguishable from regular positioning due to optical limitations in the microscopy experiment. However it is intuitively clear that when a plasmid at mid cell duplicates, the drag of a single plasmid does not change, so both plasmids will remain at mid cell since the polymer length and therefore its drag coefficient has not changed either, so it would not be able segregate the two plasmids. This is confirmed by fig. 8 where two plasmids at random initial position eventually are both positioned at mid cell. In this simulations we assumed that at the same time two plasmids are either pulled towards their nearest cell pole again governed by eq. 15, or pulled completely towards each other by a depolymerizing filament that is located in between them and attaches to both simultaneously.

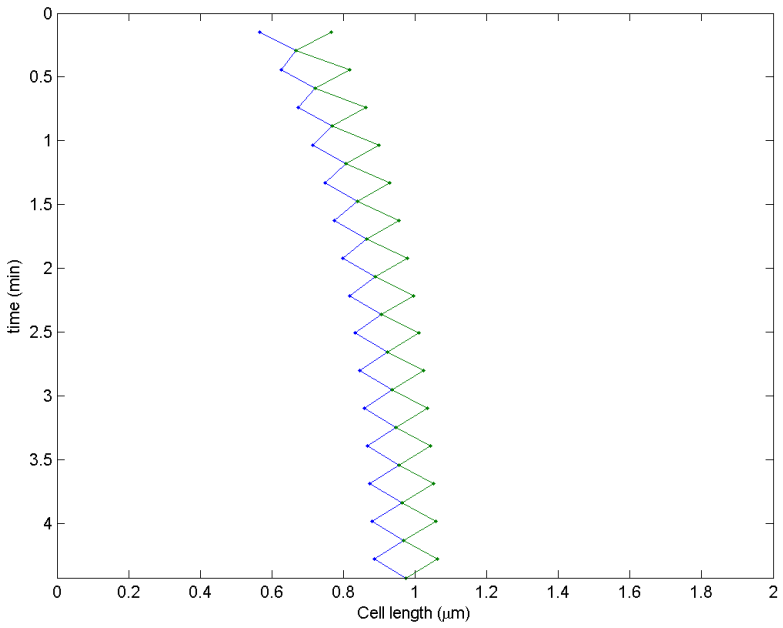

Figure 8: Plasmid trajectories in the case of $n_p = 2$ with initial position of both plasmids $x_p(0) = 0.3L$ (not shown in graph). The same parameter values are used as in fig. 7. The plasmids are both pulled towards the middle of the cell.

If however the drag coefficient would change due to an increase in ParA levels, this could influence, for instance, the bundle number and in effect separation does occur. Fig. 9 shows the trajectories of two plasmids with an increased bundle number $n = 2$ which results in segregation, but also in perpetual oscillations due to the filament that connects to two plasmids simultaneously. Therefore the plasmids meet each other half way. We conclude that plasmid partitioning does not come from single filaments pulling on plasmids with stable attachment of plasmids, due to this crucial problem.

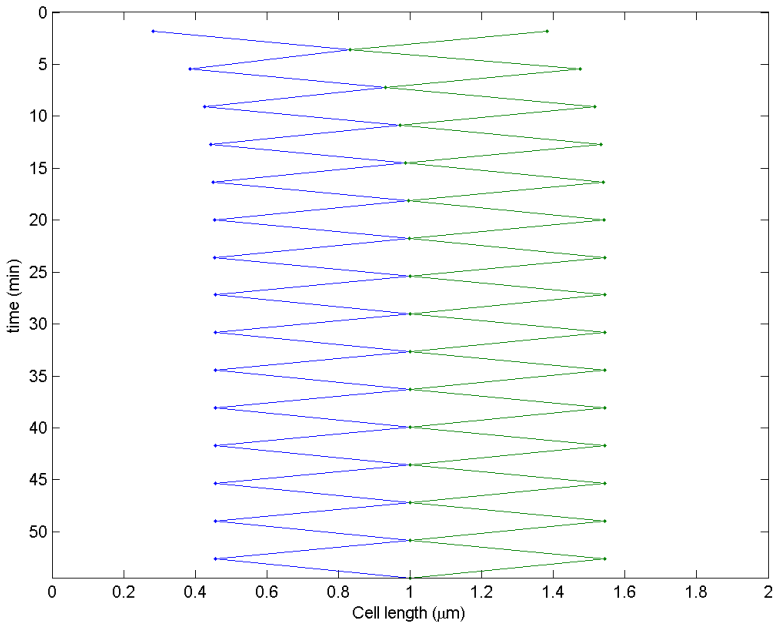

Figure 9: As in fig.8, but instead the bundle number of the ParA filaments has increased to $n = 2$ due to a hypothetical increase in ParA levels. This leads to oscillations of the plasmids.

3.2 ParA filament pulling model with ParB levels determining the detachment rate

In [1] Ringgaard *et. al.* presented a model that could explain pB171 plasmid partitioning. ParA subunits that can polymerize on the nucleoid pull on plasmids, which in turn exhibit a filament length dependent detachment rate. Kinetic

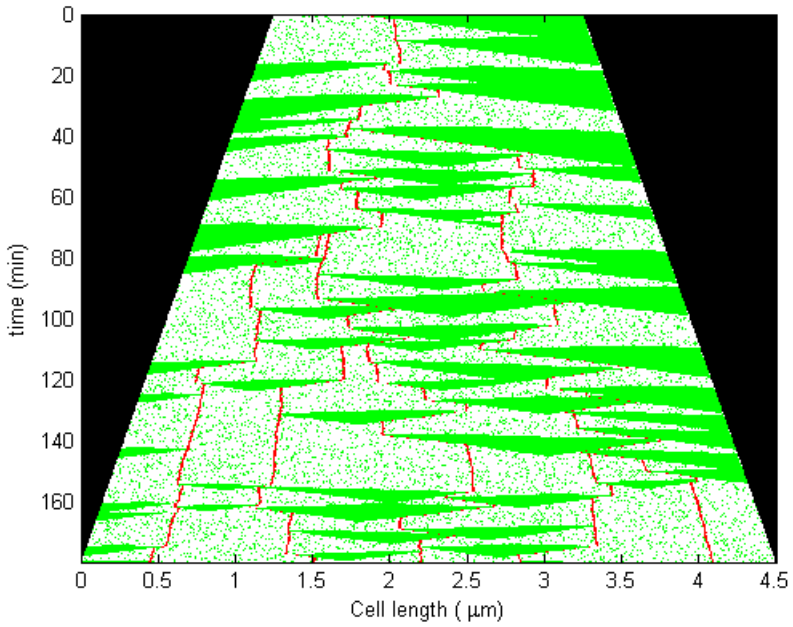

Figure 10: Kymograph of a typical outcome of one simulation. ParA is shown in green and the plasmids in red. Black indicates the region outside the cell. Time runs downwards and the cell grows in three hours of simulated time from $2\mu m$ along the long axis to $4.5\mu m$. Multiple duplication events can be observed and rapid segregation follows. The ParB levels scale with plasmid number so that plasmids exhibit a length dependent off rate. After detachment, the ParA filaments are assumed to depolymerize completely. Over time this leads to equidistant positioning in a growing cell so this mechanism generates length control.

Monte Carlo simulations showed that this could generate equidistant plasmid positioning. It remained unclear what the precise mechanism was that generates a length dependent off rate. We extended this model with ParB dynamics to explain this feature with a molecular mechanism. We hypothesized that ParB can bind nonspecifically to ParA filaments and slide along it with a high diffusion constant D on the order of $1\mu m^2/s$. If a plasmid is attached to the filament, the plasmid is supposed to absorb every ParB that slides along that polymer since the plasmids have specific binding binding sites for ParB to which ParB

molecules bind with great affinity. ParB detaches from the filament and the plasmid with a constant rate. For detailed description of the rules and code of the simulation, we refer to appendix B.1. As derived in the theory section 2.2, this mechanism can exhibit length control. It relies on two assumptions: (1) there is a critical threshold of ParB level for the plasmid above which it remains attached and (2) the ParB subunit number inside a cell scales with n_p, the plasmid copy number.

Fig. 10 shows a kymograph of a typical simulation. In a growing cell plasmids (red) are being pulled by ParA filaments (green). Repetitive cycles of attachment, pulling and detachment are observed. The ParA filaments are supposed to continue depolymerizing after detachment. This was already contained in the previous model from Ringgaard *et. al.* and it could be due to ParB molecules continuing to stimulate the ATPase after detachment of the plasmid from the polymer. However we did not model this explicitly.

Although fig. 10 shows the result of one outcome of this stochastic process, it does not say much about the average motion of the plasmid. To consider this we performed 50 simulations with two hours of simulated time and sampled the position at regular intervals of $45s$. At the site of the plasmid, at the moment of sampling, a count was added. The histogram shown in fig. 11 shows the distribution of counts summed over 50 simulations for each plasmid copy number n_p. This reflects the mean position of a plasmid as it is both a time average over one outcome of the process and an average of different outcomes. The main position in the case of one plasmid is $\frac{1}{2}L$. $L = 2\mu m$ in these simulations and the width of the distribution is about 40% of the cell size, which is comparable to the experimental data shown in fig. 3. Furthermore the histograms show that plasmids are positioned equidistantly with a spacing between the maxima that is approximately equal to $\frac{L}{n_p}$ which was predicted in the theory section 2.2.

As experiments indicated that ParB levels scale with the cell volume rather than the plasmid copy number, we incorporated this fact to see whether this mechanism could approximately give the same results as in fig. 11. The results

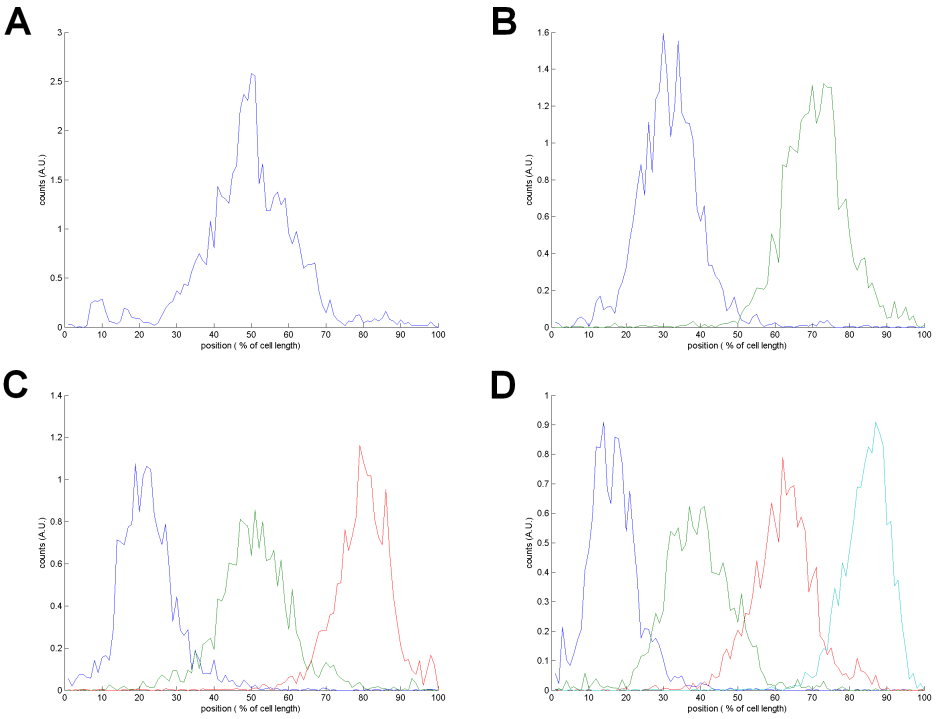

Figure 11: Histograms of the plasmid position distributions for simulations in which the ParB levels scale with the plasmid number ($B = 500n_p$). The duration of a single simulation is two hours and the length of the cell remained at $2\mu m$. At regular time intervals of $45s$ the position is sampled and a count added to that site. Summed over 50 simulations, this histograms reflect the average position of plasmids over time and over different simulations. A. One plasmid case where the plasmid locates primarily at mid cell ($n_p = 1$) B. $n_p = 2$ This histogram along with C. and D. reveal that this mechanism generates equidistant positioning of plasmids when the ParB copy number scales with n_p. C. $n_p = 3$ D. $n_p = 4$.

are shown in fig. 12. However as theory predicted this does not lead to proper plasmid segregation. This is most clearly visible in the two plasmid case, where both plasmids remain around mid cell as ParA filaments are not able to pull them apart due to a lack of increase in ParB levels after plasmid duplication. We conclude that this mechanism of ParB sliding along ParA filaments is not used by *E. coli* to position plasmids.

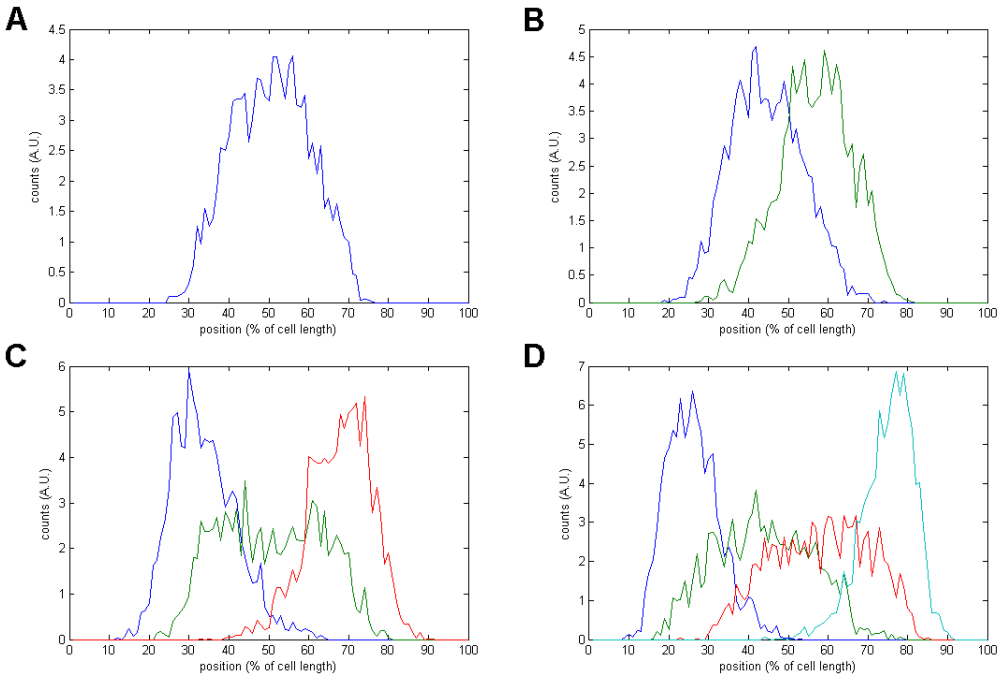

Figure 12: Histograms of the plasmid position distributions for simulations in which the ParB levels scale linearly with the cell length ($B = 500$ for $L = 2\mu m$). To see if the system could cope with this we performed 500 simulations as shown in fig. 10. Plasmid positions were sampled every $45s$ and the simulated time is three hours. Cells grow from $2\mu m$ to $4.5\mu m$. Clearly segregation now fails as there is considerable overlap between the positions of different plasmids. This is most evident in fig. B for $n_p = 2$. A. $n_p = 1$, B. $n_p = 2$, C. $n_p = 3$, D. $n_p = 4$.

3.3 Biased diffusion model

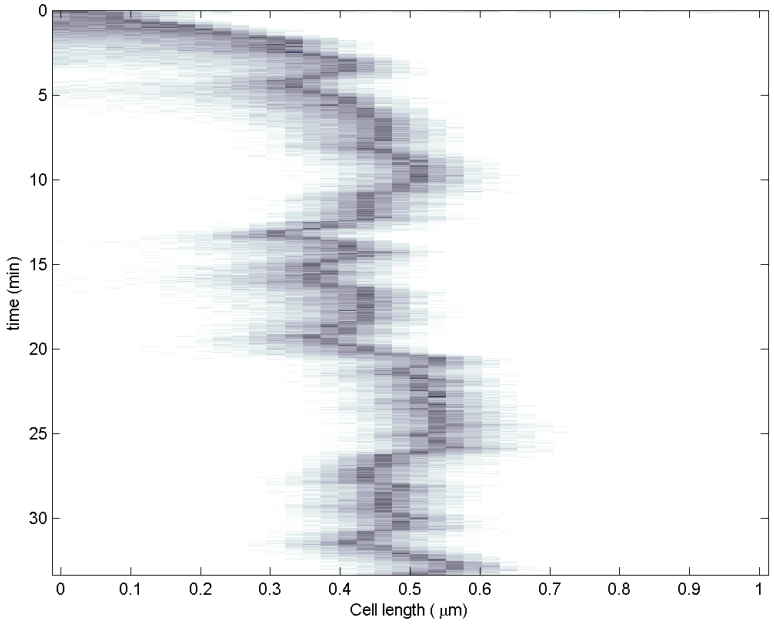

Figure 13: The ParA concentration profile along the 1D nucleoid plotted over time. High concentrations are indicated in white. At the position of the plasmid, there is a minimum in ParA concentration (darker regions). As a consequence the plasmid motion is effectively directed towards regions of higher ParA concentration as it is immobilized by ParA. The length of the simulation is $2000s$.

To verify the theory discussed in section 2.3 we performed stochastic simulations by means of a (spatial) Gillespie algorithm [27][28]. The one dimensional nucleoid was divided into different sites of length dx. Multiple cytoplasmic ParA molecules can bind to a site and diffuse to neighboring sites with diffusion constant D_A. As noted previously the plasmid can also diffuse along the nucleoid but this diffusion constant is lowered in the presence of ParA molecules at the site of the plasmid. At every site ParA can spontaneously hydrolyze and unbind from the nucleoid with rate k_A, it becomes an inactive cytoplasmic ParA. In addition at the site of the plasmid, a second hydrolysation reaction can occur with rate $k_{AB} > k_A$ in the presence of one plasmid, which reflects the stimulation of ATPase activity of ParA in presence of one plasmid at a site. After

a waiting time τ_{WT} an inactive cytoplasmic ParA, which resembles the ADP bound form of ParA, becomes active again and potent to bind the nucleoid with rate k_{on}. As this waiting time is on the order of tens of seconds, we consider the cytoplasmic concentration of cytoplasmic active ParAs uniform. In this way the fast cytoplasmic diffusion of ParAs does not have to be simulated explicitly. For detailed description of the structure of the program and the explicit rules for the diffusion rates we refer to section B.3.

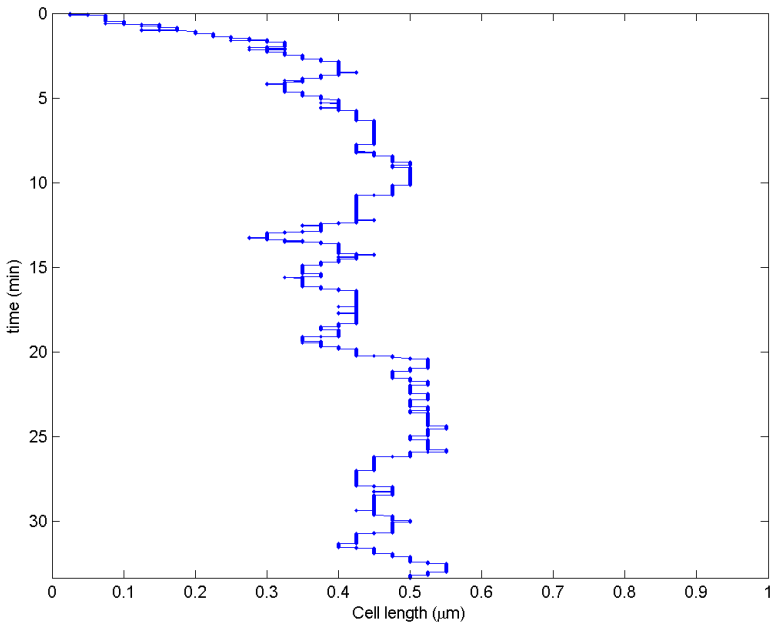

Figure 14: Plasmid trajectory plot over time of the same simulation of fig. 13. The plasmid diffuses along the long axis of the nucleoid under the influence of the local nucleoid bound ParA concentration. Net motion towards mid cell can be observed and once arrived, it remains there primarily though it can perform oscillatory motion around mid cell.

Fig. 13 shows a typical kymograph of the nucleoid bound ParA intensity profile over time. The plasmid is initially located at $x_p = 0$ and moves towards the middle of the cell. Locally at the plasmid the ParA concentration is low (darker regions), compared to regions far from the plasmid (bright). For comparison

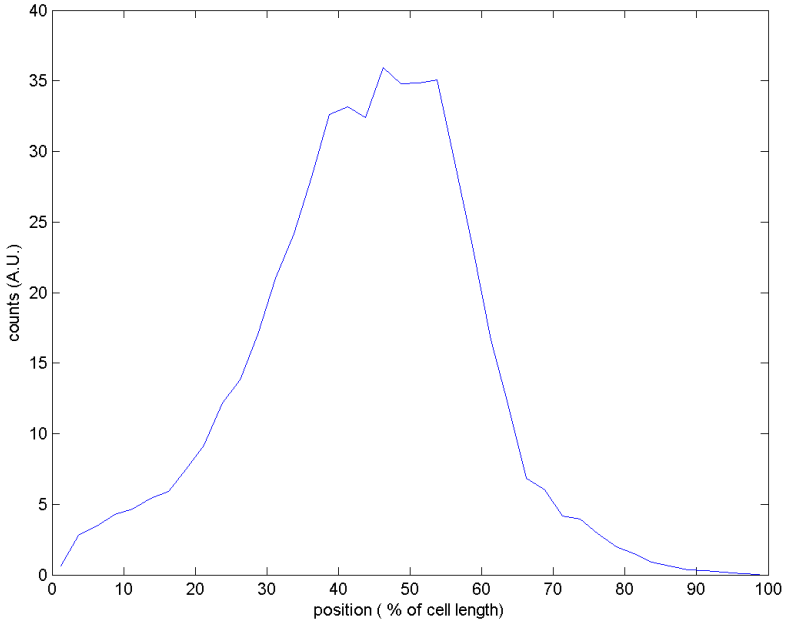

Figure 15: Histogram of the plasmid position distribution. At regular time intervals of $0.1s$ the position is sampled and a count added to that site. Summed over 50 simulations, this histogram reflects the average position of a plasmid over time and over different simulations. It can be noted that the plasmid locates primarily around mid cell.

and clarity the trajectory of the plasmid is shown in fig. 14.

Although this motion is stochastic, it does not resemble Brownian motion, but instead it is directed towards the middle of the cell. To evaluate the stochasticity we performed 50 simulations of simulated time of $2000s$ and sampled the position at regular intervals of $0.1s$. The histogram shown in 15 shows the plasmid distribution obtained in the same manner as described in the previous section. In all simulations the plasmid starts at the $-$pole: $x_p(0) = 0$. Therefore there is a slight bias in the distribution towards the left. The main position is located at $\frac{1}{2}L.$ and the width of the distribution is about 40% of the cellsize. These results have been obtained with the following parameter values: $\mathrm{d}x = 25nm$, $L = 1\mu m$, $D_A = 1.1 \cdot 10^{-3}\mu m^2/s$, $D_p = 0.1\mu m^2/s$, $k_A = 10^{-6}s^{-1}$, $k_{AB} \cdot \frac{1}{\mathrm{d}x} = 5s^{-1}$,

$k_{on} = 50s^{-1}$, $\tau_{\mathrm{WT}} = 30s$ and the number of ParA subunits (ParA_2 molecules)in the system is 5000. To ensure an initial steady state distribution the number of nucleoid bound ParA is initially 1500, distributed uniformly along the nucleoid.

Since there are major difficulties with this mechanism which are pointed out in section 2.3, we do not show any further results such as kymographs for multiple plasmids and different cell sizes.

3.4 ParA oligomer pulling model

With a biased diffusion mechanism we encountered the problem of plasmid diffusion away from the one dimensional ParA structure. In a mechanism where small ParA oligomers can diffuse and actually pull on plasmids due to depolymerization, we envisioned that we could evade the necessity of a high plasmid diffusion constant. For detailed description of the program and calculation of the rates we refer to appendix B.4.

We performed stochastic simulations where ParA oligomers of various sizes $(5 - 50nm)$ can attach to a plasmid and depolymerize completely with rate k_{AB}. Thereby it pulls the plasmid a distance equal to the oligomer length. After a waiting time τ_{WT} the oligomer can bind again from the cytoplasm to the nucleoid. We did not model the formation of oligomers explicitly.

Initially we did not take into account that the drag of the plasmid might influence the process: even though the plasmid had a zero diffusion constant (which means an infinite drag coefficient) oligomers as small as $5nm$ (approximately the length of two connected ParA subunits) were assumed to be able to pull a plasmid that distance upon depolymerization. A kymograph and plasmid trace of such a simulation is shown in fig. 16 and 17. The diffusion constant for the oligomers used in that simulation is $D_A = 0.01\mu m^2/s$ and k_{AB} is $200s^{-1}$ in the presence of 1 plasmid at the site.

Histograms obtained of simulations of 8 hours with a higher diffusion constant $D_A = 0.1\mu m^2/s$ and size $5nm$ lead to equidistant positioning, see fig. 18.

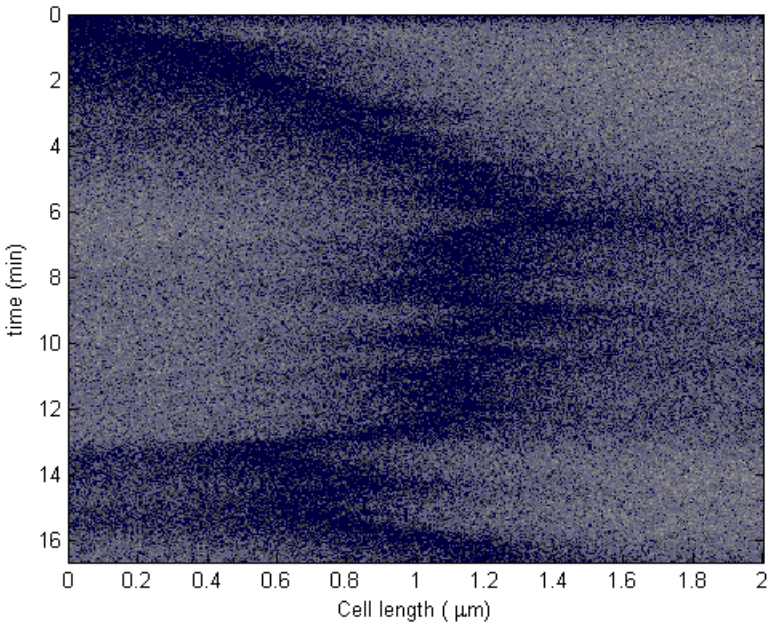

Figure 16: The ParA concentration profile along the 1D nucleoid plotted over time. High concentrations are indicated in white. At the position of the plasmid, there is a minimum in ParA concentration (darker regions). As a consequence the plasmid motion is effectively directed towards mid cell as the flux difference due to ParA oligomers diffusing in from opposing sides is minimal there. The length of the simulation is $1000s$ and the size of the oligomers $5nm$. The diffusion constant of the oligomers is $D_A = 0.01\mu m^2/s$,$k_{AB} = 25.6s^{-1}$in the presence of one plasmid at the site and the total number of ParA oligomers is equal to 2000 in this simulation.

However for a realistic mechanism we need to take the drag and diffusion of plasmids into account. It is reported that ParA oligomer sizes can be on the order of 10^2nm [16]. In theory section 2.1.1 we calculated the displacement of the plasmid as a function of $\frac{\zeta_p}{\zeta_0}$. If such an oligomer would be able to displace the plasmid $5nm$, we can estimate using eq. 15 that the plasmid diffusion constant would have to be as high as $D_p = 10^{-2}\mu m^2/s$. We performed more realistic simulations in which a plasmid could attach to oligomers of size dx with rate $k_{at} = 1000s^{-1}$ (in the presence of one plasmid) and subsequently be pulled a

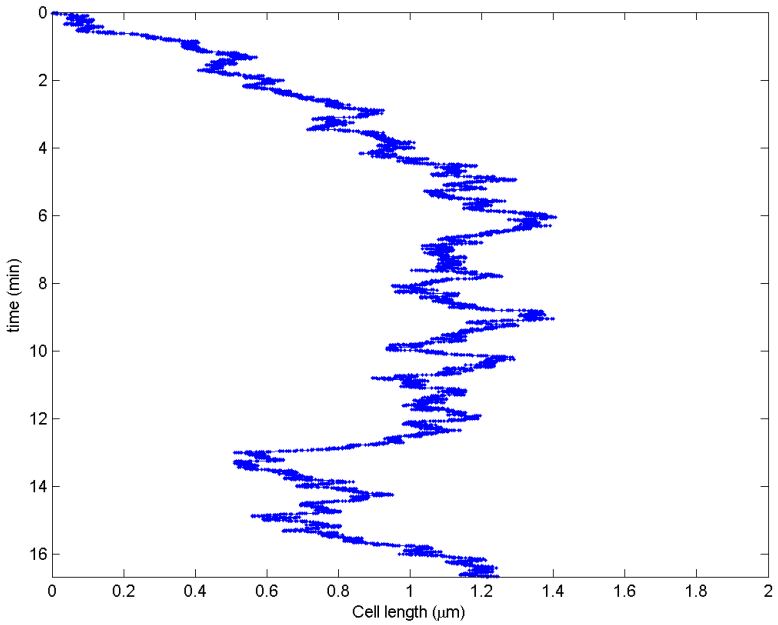

Figure 17: Plasmid trajectory plot over time of the same simulation of fig. 16. The plasmid is pulled along the long axis of the nucleoid under the influence of the local ParA oligomers who are able to diffuse on the membrane with a low diffusion constant. Net motion towards mid cell can be observed and once arrived, it remains there primarily though it can perform oscillatory motion around mid cell.

distance dx with success factor sf and rate $k_{pull} = 8s^{-1}$. Setting d$x = 100nm$ and $sf = 0.05$ this would on average mean that oligomers of size $100nm$ would pull a plasmid a distance of $5nm$. This lead again to good agreement when we set the plasmid diffusion constant to zero (results not shown).

However since oligomers of size $100nm$ would consist of several tens of ParA subunits, the amount of oligomers in the system is limited to a few hundred. Due to the waiting time a considerable amount of the ParA subunits are inactive and therefore not bound to the nucleoid. As a consequence allowing the plasmid to diffuse with constant D_p in a two dimensional embedding of the one dimensional ParA structure lead to frequent plasmid escapes. For $D_p > 10^{-4}\mu m^2/s$

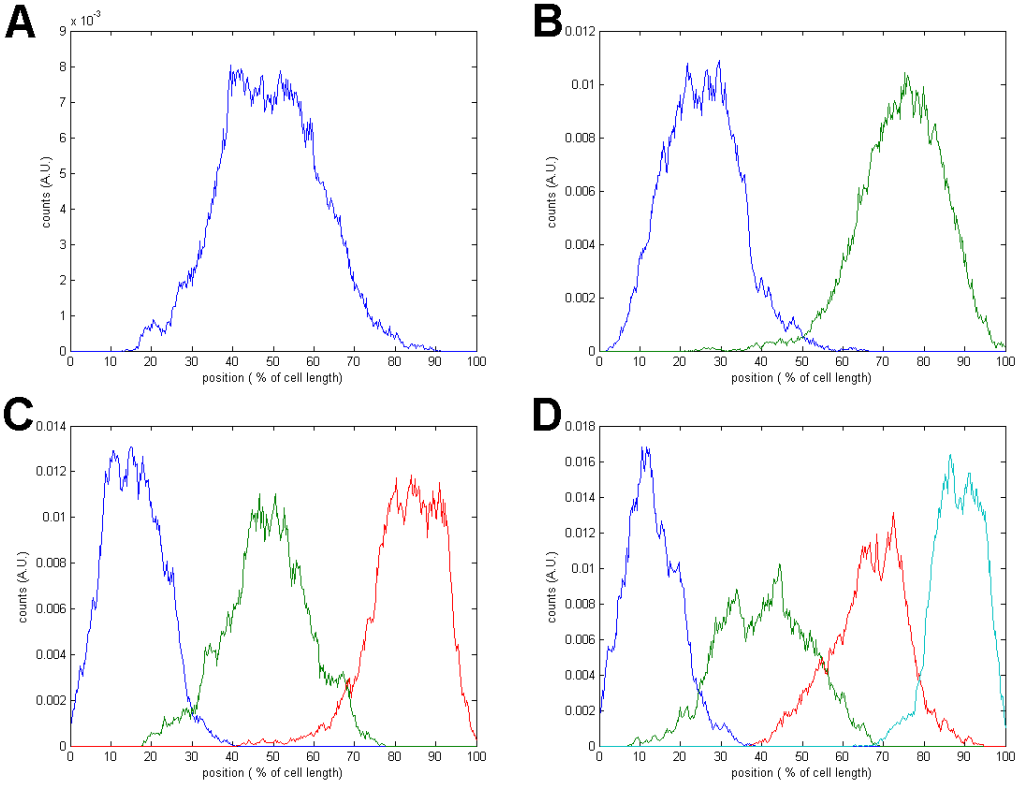

Figure 18: Histograms of the plasmid position distributions for simulations. The duration of a single simulation is eight hours and the length of the cell remained $2\mu m$. At regular time intervals of $0.1s$ the position is sampled and a count added to that site. These histograms reflect the average position of plasmids over time. However since the time that the system gets to steady state is only on the order of $10^1 s$ for this mechanism ($D_A = 0.1\mu m^2/s$ in these simulations), the initial position is of minor importance so that the sum of eight simulations of duration one hour give similar results. A. One plasmid case where the plasmid locates primarily at mid cell ($n_p = 1$) B. $n_p = 2$ This histogram along with C. and D. reveal that this mechanism generates equidistant positioning of plasmids as the peaks of the distribution have a separation of $\frac{L}{n}$. Other values of L give similar results. C. $n_p = 3$ D. $n_p = 4$.

positioning was completely abolished by the random motion of plasmid diffusion (results not shown). But we needed $D_p = 10^{-2}\mu m^2/s$ otherwise oligomers would not be able to pull plasmids as we saw before. The problem of the ne-

cessity of a high plasmid diffusion constant shows up in this mechanism as well. This also shows that a biased diffusion mechanism is very likely to fail due to the same problem. So we find it unlikely that this mechanism is used by bacteria to partition plasmids as it is not physically relevant enough for a realistic cellular environment. In the next section we explore the possibility that oligomers would spontaneously self order which could lead to more efficient pulling and tethering of plasmids.

3.5 Linear self organization of ParA

In the theory section 2.5 we explained how an Head-Tail and/or lateral affinity of oligomers could influence their spatial organization. To test whether self alignment could be achieved with parameters relevant to conditions inside a bacterial cell we performed stochastic simulations. A detailed description of the program can be found in appendix B.5 where the calculation of the propensities for the oligomer interactions are shown.

In fig. 19 a time lapse is shown of a typical simulation in which ParA oligomers (green) of size $100nm$ are initially positioned randomly on a cylinder which resembles the nucleoid surface (black). The long axis L shown horizontally is 2 micron and the circumference $3.2\mu m$. These sizes are comparable to a small *E. coli* cell. The oligomers are assumed to lie in the direction of the long axis. They can diffuse parallel to the long axis and perpendicular with $D_A = 5\mu m^2/s$. This large diffusion constant was necessary in order to obtain one long filament, rather than multiple ones. Furthermore the Head-Tail affinity between two neighboring oligomers (along the long axis) had to be around $10k_bT$ and the lateral affinity of two oligomers at the same site had to be set to $S = 1.3k_BT$. The width of a site could be varied without noticeable differences in the formation of filaments. We did not try variable oligomer sizes as we will see that this self organization turns out to be not so relevant for plasmid positioning due to other reasons explained below.

In fig. 19 we see that within several minutes oligomers form one linear structure consisting of multiple oligomers at a site ($\sim 1-10$). Both lateral and Head-Tail

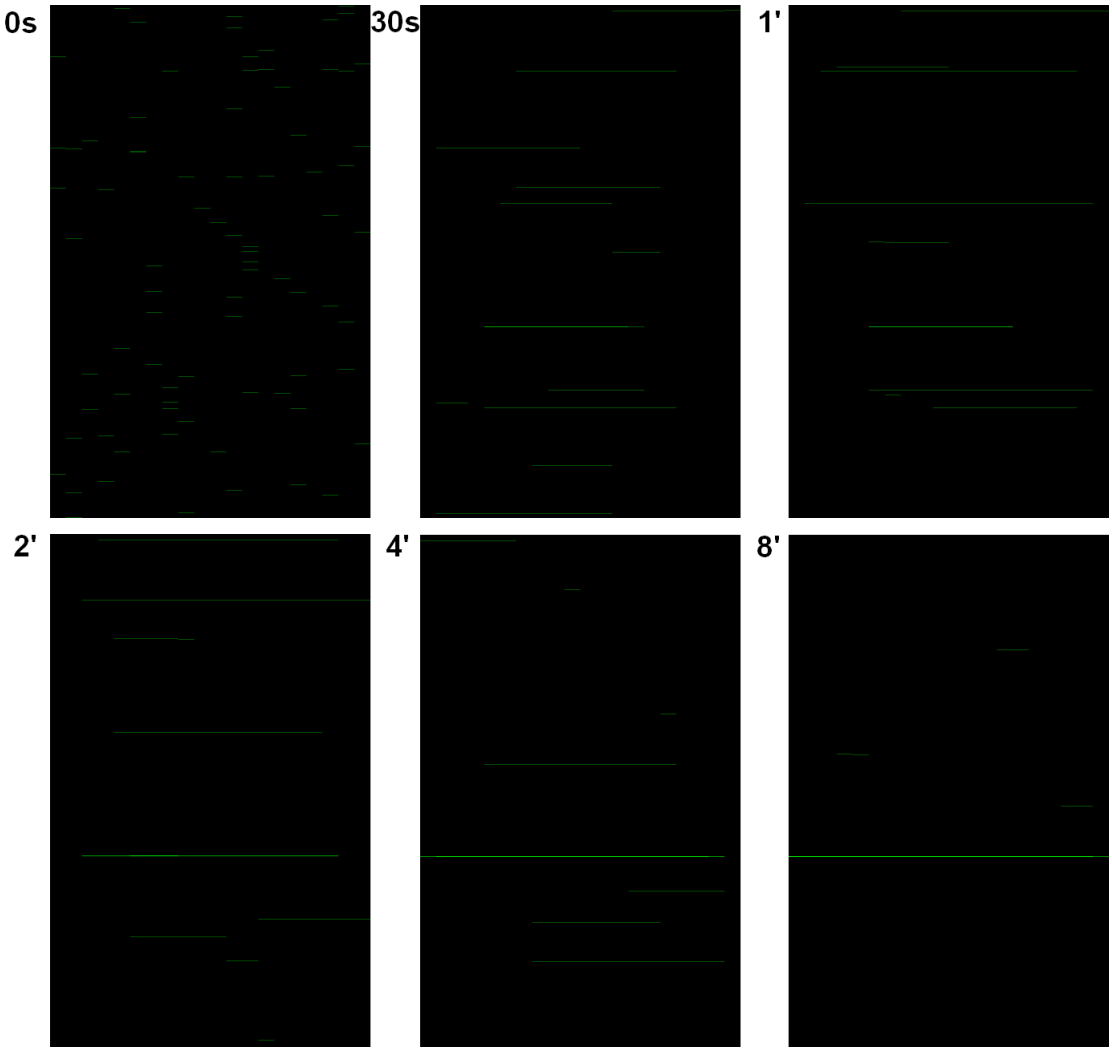

Figure 19: Time lapse of self organization of ParA in the absence of plasmids. The nucleoid (black) is a cylinder (top and bottom of square have periodic boundary conditions) and the long axis (horizontal) is $2\mu m$ in length. At $t = 0s$ 10^2 ParA oligomers (green) are positioned randomly across the nucleoid and within several minutes one stable ParA filament is formed that extends from pole to pole, similar to experiments [13].

affinity were necessary components. Setting H to zero abolished alignment and lowering S led to the formation of multiple filaments. As can be seen within the first two minutes transient filaments are formed, but due to a high diffusion rate, these structures are not stable and eventually only one filament survives

the constant rupture due to oligomers diffusing away from the filament. To see whether these self organizing oligomers could position plasmids equidistantly with a pulling mechanism we used the same rules as described in the previous section for interactions between plasmids and oligomers, though now in the presence of the interactions between the oligomers. The parameters for the oligomers were kept the same and in addition plasmids could attach with rate k_{at} and be pulled with rate k_{pull}. Again to allow for drag we introduced the success factor sf. Fig. 20 shows two kymographs of simulations in which D_p was set to zero. Since there were very few ParA outside the filament, we only show the ParA on the one dimensional structure, but one must bear in mind that this simulation was embedded on a two dimensional surface.

The parameters k_{at} was set to $1000s^{-1}$ in the presence of 1 plasmid to stabilize the plasmid as much as possible and $k_{pull} = 0.19s^{-1}$ and $sf = 0.1$ were fitted to optimize the results. One can see from the kymographs that movement is too slow (approximately $0.5\mu m/5min$) and more importantly, no new formation of opposing filaments are observed, while in experiments newly formed filaments can form and induce a change in directionality of the plasmid. In these simulations there is one filament and all ParA oligomers rapidly explore the complete nucleoid ($D_A = 5\mu m^2/s$) and eventually find the existing filament. It is very unlikely that a new ParA filament forms in the presence of an existing one, since the parameters had to be fit such that all oligomers self organize into one filament. This explains the behaviour of the simulations which is qualitatively different from experimental observations. We conclude that it is unlikely that high diffusivity of ParA oligomers on the the nucleoid can be combined with effective force exertion on plasmids.

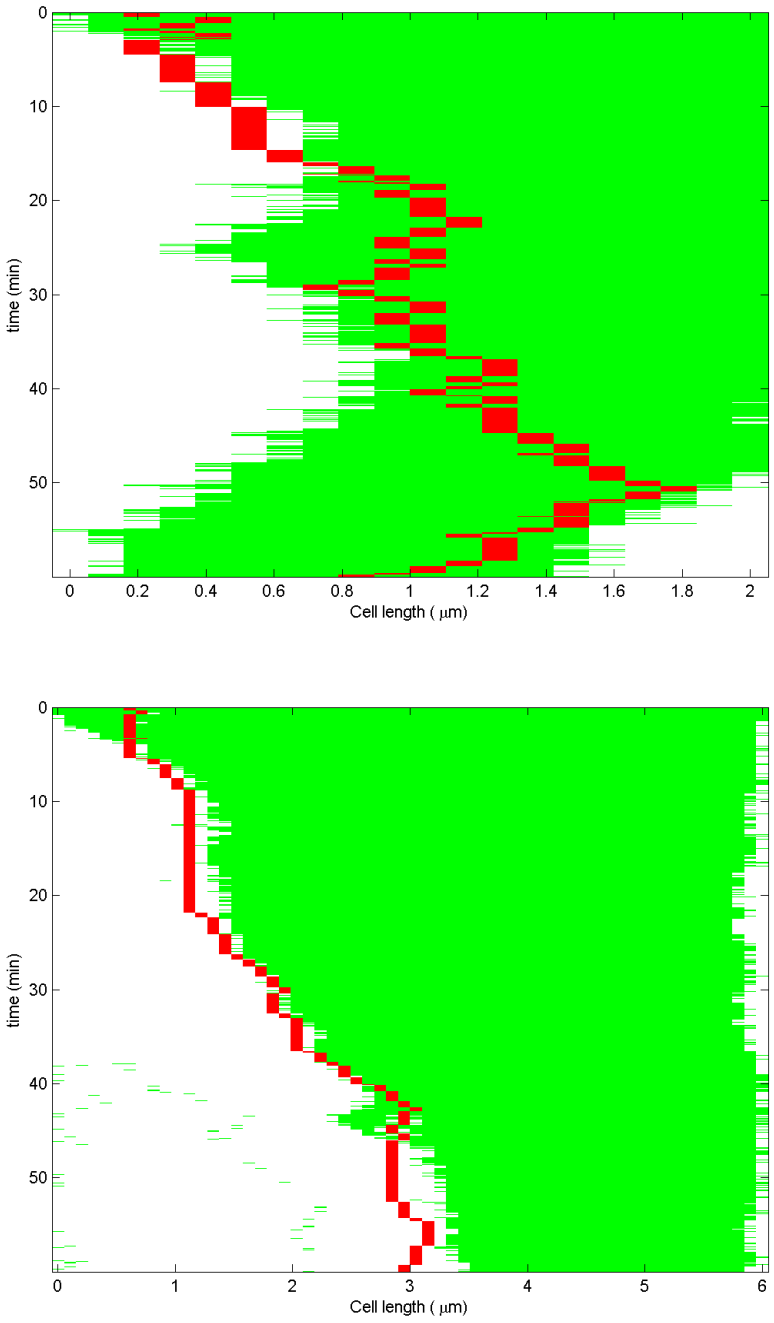

Figure 20: Kymographs of ParA oligomers pulling on a plasmid. The oligomers spontaneously self assemble into a linear structure. The parameters used are described in the text of section 3.5. ParA is indicated in green and the plasmid in red. The long axis of the cell of the upper and lower kymograph is respectively $2\mu m$ and $6\mu m$. Positioning in the middle can be observed although movement is too slow compared to experimental plasmid velocities. Also no newly formed filaments can be observed, instead the existing filament extends itself in both directions.

3.6 ParA filament pulling model with ParA sliding

In this section we report on stochastic simulations that have been performed to verify the theory developed in section 2.6. It involves the idea that ParA can form filaments by polymerizing on the nucleoid surface which is assumed to be one dimensional again. Cytoplasmic ATP bound ParA (A_{cyto}) subunits can bind to the nucleoid with rate $k_{c0} = 50s^{-1}$ [2]. We use a cytoplasmic diffusion constant to $D_A = 5\mu m^2/s$ [14] although we do not simulate the cytoplasmic diffusion explicitly for the same reason as described before, instead the concentration is assumed to be uniform. We assume the binding affinity of isolated ParA to be $B = 7k_BT$ [2]. In effect the nucleoid diffusion constant for isolated bound subunits (ParA) is then reduced to $D_A \exp\left(\frac{-B}{k_BT}\right)$.

Once a ParA has bound to a site (with gridsize $\mathrm{d}x_{\parallel} = 2.5nm$), we consider it occupied and whenever another ParA binding events occurs at that site (with rate $k_{c1} = 170s^{-1}$ because of cooperative binding [2]), The newly bound ParA will be in a form (AS) that is able to diffuse along the filament (with constant D_A) until it encounters an empty site at which point it be converted to a nucleoid bound subunit instantaneously because of the affinity for DNA. As soon as two neighbouring sites are occupied the nucleoid diffusion constant of both subunits is set to zero because of assumed polymerization. In this way we can ensure that new polymers will be formed by new attachment of either direct binding to the nucleoid or binding to the filament and subsequently sliding to the tip ends.

ParA subunits can hydrolyze and unbind spontaneously with a rate $k_{off} = 0.2s^{-1}$ but only when there is at most one neighboring bound ParA. If both neighbouring sites are occupied, the ParA is not at the tip of the polymer and therefore it cannot unbind spontaneously. For simplicity we do not allow AS to unbind spontaneously since with the high diffusion constant it will surely find an empty site rapidly before unbinding due to the differences in rates.

The plasmid is assumed to be immobile and the attachment event of a plasmid to a ParA subunit is the same as described in the previous section with the same

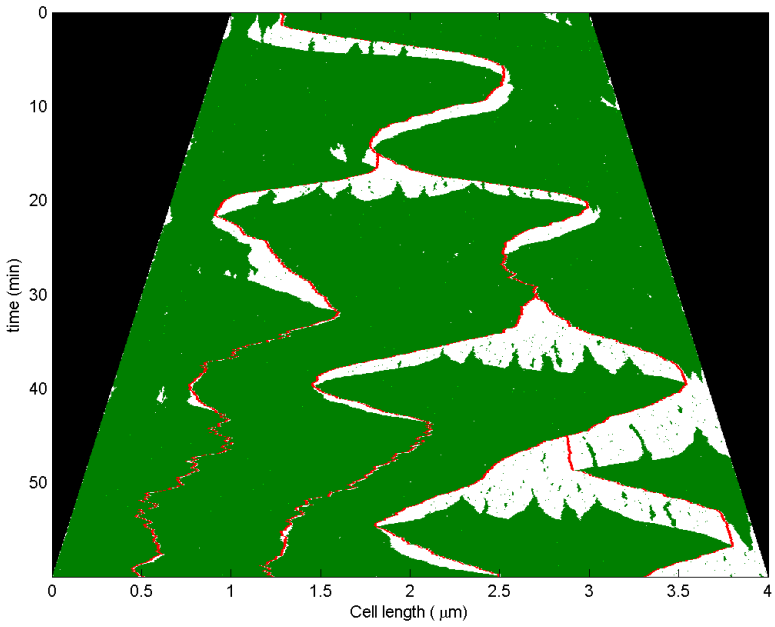

Figure 21: Kymograph of a typical outcome of one simulation. ParA is shown in green and the plasmids in red. Black indicates the region outside the cell. Time runs downwards and the cell grows in one hour of simulated time from $2\mu m$ along the long axis to $4\mu m$. Multiple duplication events are followed by rapid segregation and oscillatory motion of both the ParA distribution and the plasmid. The cell initially contains one plasmid and at the end of the simulation four plasmids. A lack of a newly formed opposing filament induces overpulling as can be seen near the +pole after 30 minutes. Over time the motion of newly formed polymers catches up which leads to equidistant positioning in a growing cell. This mechanism therefore generates length control.

rate $k_{at} = 1000s^{-1}$ in presence of one plasmid at the site. It cannot bind to an AS molecule. Once attached the depolymerization event can occur with rate $k_{pull} = 25.6s^{-1}$ and success factor $sf = 0.35$. In effect the ParA is converted into the state Timer, which reflects the inactive cytoplasmic ADP bound form. With rate $1/\tau_{\mathrm{WT}}$ the activation to A_{cyto} occurs. We set $\tau_{\mathrm{WT}} = 20s$ to allow for the slow activation of ATP bound ParA [2]. The total number of ParA units is set to be such that every site can be occupied: Total ParA$= \frac{L}{\mathrm{d}x_{\parallel}}$. This means

that we assume that ParA exhibits a constant density throughout the cell cycle like in the case of ParB (fig. 3).

We explored various other parameter values: lowering D_A to $0.1\mu m^2/s$ or increasing the subunit size to $dx = 20nm$ do not influence the results. As long as $k_{c1} > k_{c0}$ the cooperativity is ensured and resulting positioning is unaffected although less oscillations can be seen as k_{c1} decreases to k_{c0}. Increasing the off rate to values above $0.5s^{-1}$ induces a lack of spontaneous formation of ParA filament. Increasing τ_{WT} leads to fewer available ParA molecules and therefore slows down the process. This can be counterbalanced if the density of ParA in the system was increased.

Fig. 21 shows a typical kymograph of a simulation where plasmids are dynamically positioned by polymerizing and retracting ParA polymers as the cell grows. Multiple duplication events occur followed by rapid segregation and positioning. This model positions the plasmids most precisely in the presence of two opposing filaments present. If there is only one polymer present due to a lack in spontaneous nucleation a plasmid will be overpulled, resulting in oscillations of both ParA and the plasmid. This can be seen in the kymograph from $30min$ onwards near the +pole.

Histograms A. and B. shown in fig. 22 are obtained by performing 50 simulations of two hours simulated time in which cells grow from $2\mu m$ to $3\mu m$. Initially the cell starts with one plasmid and after an hour a duplication event occurs. In 50 other simulations the cell starts with three plasmids and after 60min one of the plasmids duplicates. Equidistant positioning can be observed.

We also performed control simulations in which the ParA binding along the filament was inhibited and therefore sliding did not occur. This resulted in immobility of the plasmid for a large regime of parameter values including the ones described above. This suggests that when the copy number of polymerizing subunits is limited, direct cytoplasmic binding might not be sufficient to ensure rapid polymerization. Increasing the density of the ParA in the system to $2 \cdot \frac{L}{\mathrm{d}x_{\|}}$

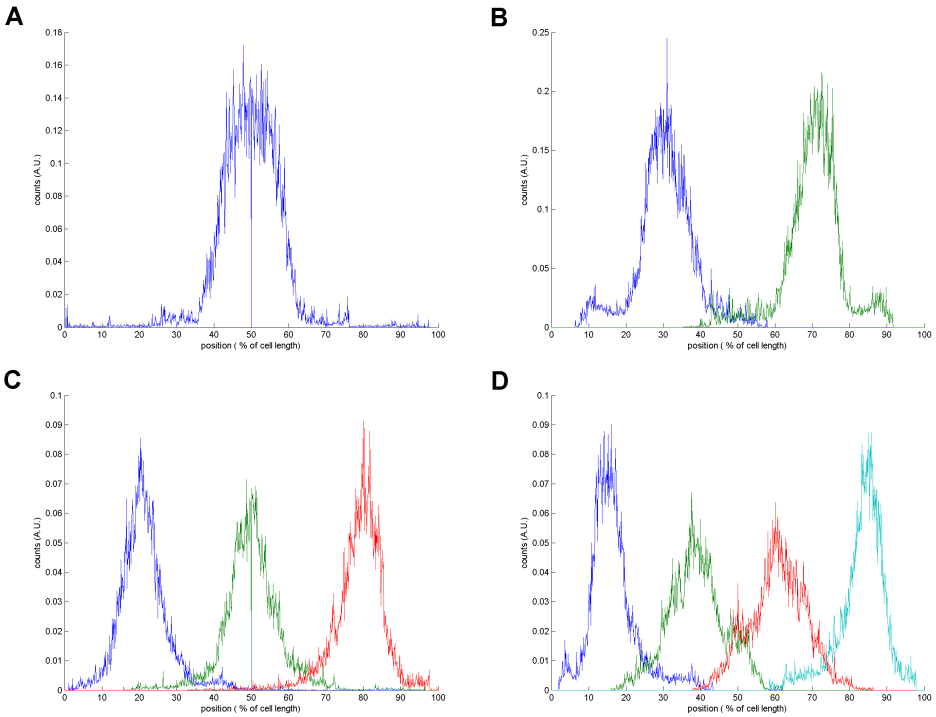

Figure 22: Histograms of the plasmid position distributions for simulations in which the ParA subunits can bind and slide along length of the ParA filaments. The duration of a single simulation is two hours and the length of the cell increased from $2\mu m$ to $3\mu m$. At regular time intervals of $1s$ the position is sampled and a count added to that site. These histograms reflect the average position of plasmids over time and outcome of the stochastic process. In 50 simulations the initial plasmid number is $n_p = 1$ and increases after one hour to two by a duplication event. The position histogram in A. ($n_p = 1$) is obtained by considering the position in the first hour of a simulation. Likewise in the second hour the position of two plasmids are considered, resulting in B. ($n_p = 2$). In 50 other simulations of two hours, the n_p is initially three and increase to four in the same manner as described above. In this way we obtain the graphs in C. ($n_p = 3$) and D. ($n_p = 4$). The exact moment for duplication is irrelevant for the mechanism, but in this case it is merely chosen in the middle of the simulation in order to obtain equal time average statistics.

solved the problem of insufficient pulling events, but in effect no equidistant positioning could be observed. Instead the plasmid exhibited random bidirectional motion, which confirms that the sliding provides the the length control.

Although some oscillations in the ParA distribution can be observed, this mechanism predicts that this is only a small effect. In the experimental data, it is not clear whether ParA oscillations without plasmids following the filament are more common observations than as seen in this model. We did not take into account the effects of drag combined with subunits sliding along the filament length. Potentially this could create more ParA oscillations without pole to pole movement of plasmids when short ParA filaments get reeled resulting in complete disappearance of ParA.

Lastly since this model involves polymerization, it has the potential to explain the experimental observations of ParA filaments extending into the cytoplasm away from the nucleoid to recruit cytoplasmic plasmids to the nucleoid region. Therefore we favour this model over the biased diffusion model. In principle self-organizing oligomers could achieve this as well, however this model has other severe problems described in section 3.5. The ParB sliding mechanism was falsified experimentally, therefore this model is currently most satisfactory.

4 Discussion and Conclusion

In this Masters thesis we looked at various mechanisms for pB171 plasmid segregation in *E. coli*. The five key components are [29]: (1) ParA, a Walker type ATPase that forms linear structures *in vivo* on the nucleoid (2) and (3) ParB, a DNA binding protein that targets (4) *parC* on plasmid pB171 and stimulates the ATPase activity of ParA in the presence of ATP(5). Recently two ideas have been proposed for this type Ib segregation mechanism, but it remained unclear whether they could generate the observed equidistant positioning and segregation of low copy number plasmids. Firstly, a scenario in which ParA polymerizes on the nucleoid and starts to depolymerize upon encounter of a plasmid due to the stimulation of the ATPase activity by ParB has been shown to generate ap-

propriate positioning with the assumption that the plasmid detachment rate is dependent on the length of the filament upon attachment [1]. ParA polymerization in pB171 is shown *in vitro* [15] [16] [6]. Secondly, Vecchiarelli *et. al.* recently proposed a model where plasmid diffusion is biased towards high concentration levels of ParA as they immobilize it due to their attachment to the nucleoid which serves as a scaffold [2]. As ParB enhances the detachment of ParA from the nucleoid this concentration is dynamic and would bias the position of the plasmids. We investigated both ideas theoretically and with stochastic simulations. In addition we report on a third mechanism which is a combination of the two: ParA can oligomerize to short filaments that can both diffuse on the nucleoid surface and pull on plasmids by depolymerization.

ParA polymerization and depolymerization on their own insufficient to answer the question whether plasmids can be partitioned appropriately. The stability of the connection between a plasmid and ParA turns out to be of major importance. Starting with the assumption that plasmids remain stably attached to the filament due to a stable ParA-ParB interaction, we can conclude that this will not be able to position two plasmids equidistantly since oscillations will give the wrong time averaged distributions. If we relax this assumption by allowing repetitive connection and disconnection so that two filaments can pull on it consecutively, the influence of drag would rely strongly on the assumption that the total ParA copy number level inside a cell depends on the plasmid copy number and not on the cell volume. However since ParB levels scale rather with cell volume and ParA and ParB lie on the same operon this assumption does not seem likely. Experimental verification is needed in this case. Another argument against this mechanism is the experimental indication that the DNA binding affinity of P1 ParA is several k_BT by comparing the DNA binding and unbinding rate [2]. This binding increases the filament drag sufficiently such that even short ParA filaments induce considerable plasmid motion. It would be essential that two opposing filaments are present in close proximity of the plasmid all the time to pull in opposite directions, otherwise a plasmid is rapidly pulled to a cell pole. However experimentally oscillations of ParA are also observed. This indicates that in reality the mechanism should be robust enough to deal with

the presence of only one filament for several minutes as plasmid displacement all the way to a pole is not observed experimentally. Therefore we do not currently favour this mechanism.

To explain the length dependent detachment rate of the ParA polymer pulling model in [1] we assumed that ParB molecules can bind anywhere along the length of the filaments and slide rapidly along it. An attached plasmid can then "absorb" the ParB as it has several DNA binding sites for this protein. The number of ParB molecules is then assumed to be critical for the stability of the filament-plasmid connection. This model can generate equidistant positioning with the assumption that the ParB copy number in a cell scales with the plasmid number, not with the cell volume. However experiments indicate that the latter is the case, which abolishes segregation.

Instead of assuming that ParB can bind along the filament, we considered the possibility of ParA subunits binding along the length of the ParA filament and sliding rapidly to the tip ends where they attach to it. In effect the ParA polymerization rate of the ParA filaments is dependent on this length. No strong assumptions have to be made on the ParA levels: a fixed ParA density is sufficient, which is likely to be the case as ParA and ParB lie on the same operon and ParB exhibits a fixed density. However experiments on the ParA levels need to be performed to verify this assumption. This mechanism could generate equidistant positioning with high precision. The influence of motion due to changing drag of filaments decreasing in size could be beneficial in this mechanism, but it works even with the assumption that ParA is strongly bound to the nucleoid, resulting in a small $\frac{\zeta_p}{\zeta_0}$ even for short filaments.

A biased diffusion mechanism can generate regular positioning, but requires the assumption of a high plasmid diffusion coefficient. However [19] reports on a low diffusion coefficient and confinement of plasmids in absence of a partitioning system. More stringently the diffusion of the plasmid would have to be confined to the linear structure of ParA embedded on the surface of the nucleoid which is highly unlikely. Therefore the problem of plasmids wandering off from

the filament seems too severe.

As an alternative we studied a new model which bridges the gap between the biased diffusion and polymer pulling scenarios: oligomers diffusing and depolymerizing upon encounter with a plasmid which thereby exert force on plasmids. This model aims to benefit from the diffusion components which induce automatic equidistant positioning without the necessity of plasmid diffusivity. However diffusive oligomers are not able to exert force efficiently on a relatively high drag object like the plasmid. By the Einstein relation we conclude that we need a high diffusion constant to ensure that the plasmid drag is low enough for oligomers to induce motion, which leads back to the same problem. Assuming a lower ParA diffusion constant inhibits timely positioning as the dynamic formation of the ParA concentration is formed on too long timescales. Self organization of oligomers into filamentous structures by means of Head-Tail and lateral interactions that result in more effective pulling would not require a high diffusion constant of the plasmid. Therefore it has the potential to solve the problem of plasmids wandering away from the ParA filaments. However the self organization simulations show qualitatively the wrong behaviour of the ParA distribution: no ParA oscillations can be observed in contrast to experiments [13].

We propose that ParA polymers that pull on plasmids can be a realistic mechanism that generates equidistant positioning of pB171 plasmids. It requires the assumption that the polymer growth rate depends critically on the rate of subunits sliding into the tip. The reason this is essential comes from two facts: (1) the copy number of the ParA is in bacterial cells is limited to few thousands ([6], [4], *personal comments* F. Szardenings and M. Roberts) and (2) the rate from (ParA-ADP)$_2$ to (ParA-ATP)$_2$ is rate limiting. It takes at least tens of seconds before ATP bound ParA can interact with other ParA and bind to the nucleoid. As a consequence only very few cytoplasmic ParA subunits are available to ensure polymerization. The sliding along the filament seems to speed up the process of supplying ParA subunits for filament elongation as sliding knock out simulations did not allow for timely positioning in a large regime of

parameters. This problem could be prevented by increasing the density of ParA in the system, but instead of equidistant positioning, this led to random positioning. Rapid one dimensional diffusion of subunits along polymers to ensure a high polymerization rate might be occurring in several other types of polymers such as microtubule or actin, however the effect of it can easily be obscured in the presence of high enough subunit concentrations and rapid conversion of the NDP to NTP bound form which renders cytoplasmic diffusion with the observed rate of $7\mu m^2/s$ sufficient.

Lastly since the nucleoid surface is spatially extended and polymers are one dimensional we require some sort of linear organization of the nucleoid. Some groups have reported this [23][24] but it is not completely understood if and how the nucleoid shape is organized throughout the cell cycle. ParA forms helical structures *in vivo* [13] on the nucleoid with a spacing on the order of a micron. Whether this formation occurs at a sort of "railway track" presumably due to the shape of the nucleoid remains unclear. However if we allow for spontaneous formation of polymerization this leads to the problem that multiple long filaments could form and position plasmids simultaneously. What mechanism might address this problem requires further investigation by two dimensional modelling. Also although unlikely the possibility of a high plasmid diffusion constant could disrupt the mechanism as the connection between the filament and plasmid cannot be too stable as it would induces repetitive plasmid oscillations. Once detached however, a high diffusivity would induce quick movement away from ParA filaments and thereby a complete randomization of the plasmid position. Low diffusivity ensures that the distance moved away from filaments is low and therefore the randomizing effect might be small. In this way ParA polymers could position plasmids equidistantly.

A Methods - Theory

A.1 Trajectories of a plasmid pulled by one depolymerizing filament

We want to obtain the position of the plasmid over time when it is pulled by one filament bundle. ζ_p is the drag coefficient of the plasmid, assumed to be time independent. ζ_A is the drag coefficient of the ParA filament bundle. As noted in the main text the equation of motion comes from Newton's third law in a viscous medium:

$$\zeta_p \vec{v}_p = -\zeta_A \vec{v}_A$$

k_d is the depolymerization rate, k_p the polymerization rate, a is the size of a ParA subunit, n is the number of ParA filaments that a ParA filament bundle consists of. ζ_0 is the drag coefficient of one ParA subunit. The motion of the components is induced by a bundle of ParA filaments depolymerizing at the point of connection between plasmid and filament. We assume that the depolymerization occurs at the tip of every protofilament and that one protofilament does not shrink more quickly than the others so that n ParA subunits have to be depolymerized from the tip before the plasmid effectively has moved a distance a. This is the case in microtubule depolymerization. In effect the plasmid and centre of mass of the filament move towards each other, so the velocities are related by the following constraint:

$$|\vec{v}_p - \vec{v}_A| = \frac{ak_d}{n}$$

Taking into account that the velocities of the two components are in opposite direction this results in the following e.o.m.:

$$v_p(t) = \frac{\zeta_A(t)\ \frac{ak_d}{n}}{\zeta_p + \zeta_A(t)} \tag{12}$$

The drag coefficient of the filament is proportional to the number of subunits in it:

$$\zeta_A = \zeta_0 \left(\frac{nl_0}{a} - (k_d - k_p)t \right) \tag{13}$$

Inserting this expression into the e.o.m. 12 and integrating over time results in the position of the plasmid:

$$x_p(t) = x_p(0) + \frac{ak_d}{n}\left(t - \frac{\frac{\zeta_p}{\zeta_0}}{k_d - k_p}\ln\left[\frac{\frac{\zeta_p}{\zeta_0} + \frac{nl_0}{a}}{\frac{\zeta_p}{\zeta_0} + \frac{nl_0}{a} - (k_d - k_p)t}\right]\right)$$

We can take several limits to interpret the result in comprehensible cases:

$$\lim_{\frac{\zeta_p}{\zeta_0}\nearrow\infty} x_p(t) = x_p(0) + \frac{ak_d}{n}\left(t - \frac{1}{k_d - k_p}\left[\frac{nl_0}{a} - \left(\frac{nl_0}{a} - (k_d - k_p)t\right)\right]\right) = x_p(0) \tag{14}$$

When the plasmid is much heavier than the filament, no pulling will occur, instead the filament gets reeled in.

$$\lim_{\frac{\zeta_p}{\zeta_0}\searrow 0} x_p(t) = x_p(0) + \frac{ak_d t}{n}$$

When the plasmid is much lighter, it will be pulled with the maximum velocity $\frac{ak_d}{n}$, the filament remains stationary.

$$\lim_{k_p\nearrow k_d} x_p(t) = x_p(0) + \frac{ak_d t}{n}\left(\frac{\zeta_0\frac{nl_0}{a}}{\zeta_0\frac{nl_0}{a} + \zeta_p}\right)$$

When the filament grows as quickly as it shrinks, the filament length remains l_0 and the velocity of the plasmid will be proportional to the fraction of the drag of the filament and total drag. Now we look at the position of the plasmid in the limit of a completely depolymerized filament:

$$\lim_{t\nearrow\frac{nl_0}{a(k_d-k_p)}} x_p(t) = x_p(0) + l_0\frac{k_d}{k_d - k_p} - \frac{\frac{\zeta_p}{\zeta_0}ak_d}{n\,(k_d - k_p)}\ln\left[\frac{\frac{\zeta_p}{\zeta_0} + \frac{nl_0}{a}}{\frac{\zeta_p}{\zeta_0}}\right]. \tag{15}$$

When $\zeta_p \approx \zeta_0 nl_0/a$, we obtain a displacement of the plasmid that depends linearly on l_0:

$$\Delta x_p = l_0\frac{k_d}{k_d - k_p} - \frac{\frac{\zeta_p}{\zeta_0}ak_d}{n\,(k_d - k_p)}\ln 2. \tag{16}$$

Displacements in eq. A.1 for relevant parameter values are listed in table 1.

If $k_d \leq k_p$, the filament continues to extend to the +pole upon depolymerization, so the following relation holds:

$$\zeta_A(t) = \zeta_0 n\left(\frac{L - x_p(t)}{a}\right)$$

Inserting this in eq. 12 results in the following differential equation:

$$v_p(t) = \frac{k_d\,(L - x_p)}{\frac{\zeta_p}{\zeta_0} + \frac{(L-x_p)n}{a}} \tag{17}$$

From eq. 17 we can infer that the velocity remains positive until it reaches the +pole eventually. The question is whether that happens within the relevant timescales. If initially pulling is quick but slows down considerably in the middle of a cell because shorter filaments cannot exert high enough force this generates length dependent pulling effectively. Here we show that this cannot hold. If the plasmid is effectively pulled to the middle in a big cell of $L_{max} = 3.5\mu m$ due to a considerable decrease in velocity to values around $1nm/s$ at $\frac{1}{2}L_{max}$, it will surely not pull it to the middle timely in a small cell of $L_{min} = 2\mu m$ because a filament of length $l_0 = \frac{1}{2}L_{max} = \frac{7}{8}L_{min}$ is reeled in too much. To make this argument precise we note in the e.o.m. 17 that $v_{max} = k_d a$. In the middle of a cell we need slowing down to velocities on the order of $1nm/s$ to prevent overpulling. For a lower bound of $v_{max} = k_d a = 4s^{-1} \cdot 2.5nm = 10nm/s$, we would need $\zeta_p/\zeta_0 = 4 \cdot 10^3$ in a cell of length L_{max} to obtain this tenfold reduction in speed when a plasmid at $x_p = 0.7L_{max}$ is being pulled towards the +pole.

The solution to this equation involves the so called Lambert W function, which is the inverse function of $g(W) = We^W$:

$$x_p(t) = L - \frac{a}{n}\frac{\zeta_p}{\zeta_0}\; W\left[\frac{\exp\left(\frac{-k_d t}{\frac{\zeta_p}{\zeta_0}} + \frac{d_1}{\frac{\zeta_p}{\zeta_0}} - 1\right)}{\frac{\zeta_p}{\zeta_0}}\right]. \tag{18}$$

d_1 is the integration constant that is dependent on the initial condition. After fixing parameter values, d_1 was obtained numerically in Mathematica by setting $x_p(0) = 0$ and consequently the trajectory x_p was obtained. We set $k_d = 4s^{-1}$, $a = 2.5nm$, $L \in \{L_{min}, L_{max}\}$ and we varied $\frac{\zeta_p}{\zeta_0} \in \{10^1, .., 10^6\}$.

For $\frac{\zeta_p}{\zeta_0} \leq 10^3$, timely pulling could be achieved: $x_p(t = 10min) \geq \frac{1}{2}L$. But we need at least a drag ratio of $\zeta_p/\zeta_0 = 4 \cdot 10^3$ to get reduction in plasmid velocity at mid cell. Inspecting the trajectory for this ratio leads to the result that it takes about $13min$ to pull a plasmid $1\mu m$, from $-$pole to the centre in a cell of length L_{min}, which is too long compared to experimental values:

$x_p(t = 10min) = 0.8\mu m$ and $x_p(\widetilde{t}) = \frac{1}{2}L_{min} \Rightarrow \widetilde{t} \approx 13min.$ A typical trajectory is plotted in fig.23.

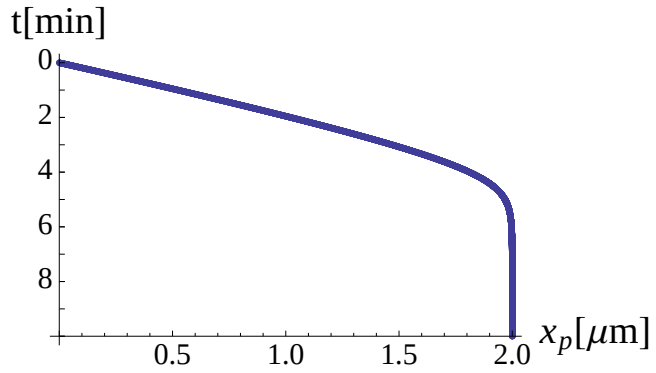

Figure 23: Plot of plasmid trajectory given in eq. 18 ($\zeta_p/\zeta_0 = 100$, $L = L_{min}$) as it is pulled along by a filament that is constantly extending to the cell pole due to rapid polymerization at the +pole tip end. With this drag ratio the plasmid is most of the time displaced with a rate that is nearly maximal ($v_{max} = 10nm/s$).

A.2 Trajectories of a plasmid pulled by two depolymerizing filaments

We proceed with setting up the e.o.m. for a plasmid that is pulled by two ParA filament, A_- extending to the $-$pole of a cell and A_+ extending to the +pole. Let l_- and l_+ be the respective initial filaments lengths, and n_-, n_+ the number of filaments in the bundles. W.l.o.g. $n_-l_- < n_+l_+$. The extension to two filaments leads to the following e.o.m:

$$\begin{aligned} &\zeta_p\vec{v}_p = -\zeta_{A_-}\vec{v}_{A_-} - \zeta_{A_+}\vec{v}_{A_+} \qquad n_-l_- < n_+l_+ \Rightarrow \\ &\zeta_p v_p = -\zeta_{A_-}v_{A_-} + \zeta_{A_+}v_{A_+} \end{aligned} \tag{19}$$

The fixed depolymerization rates give the following constraints by taking into account the directions of the velocities since ($n_-l_- < n_+l_+$):

$$\begin{aligned} \left|\vec{v}_p - \vec{v}_{A_-}\right| = \frac{ak_d}{n_-} \quad &\Rightarrow\ v_{A_-} - v_p = \frac{ak_d}{n_-} \\ \left|\vec{v}_p - \vec{v}_{A_+}\right| = \frac{ak_d}{n_+} \quad &\Rightarrow\ v_{A_+} + v_p = \frac{ak_d}{n_+} \end{aligned} \tag{20}$$

Similar to the one filament situation, this is under the assumption that all protofilaments in a particular bundle depolymerize equally fast and that de-

polymerization only occurs at the tip of the bundle. Lastly we introduce again the drag coefficients of the ParA filaments that depend on the number of ParA subunits:

$$\zeta_{A_-} = \zeta_0 \left(\frac{n_- l_-}{a} - (k_d - k_p)t \right)$$
$$\zeta_{A_+} = \zeta_0 \left(\frac{n_+ l_+}{a} - (k_d - k_p)t \right).$$

After insertion of this expression together with eq. 20 into eq. 19 and integrating that equation over time we obtain the following result:

$$x_p(t) = x_p(0) + a k_d t \left(\frac{1}{n_+} - \frac{1}{n_-} \right) + \ln \left[\frac{\frac{\zeta_p}{\zeta_0} + \frac{n_+ l_+ + n_- l_-}{a}}{\frac{\zeta_p}{\zeta_0} + \frac{n_+ l_+ + n_- l_-}{a} - (k_d - k_p)t} \right] \frac{k_d}{k_d - k_p} \left(l_+ - l_- + a \left(\frac{1}{n_+} - \frac{1}{n_-} \right) \left(\frac{\zeta_p}{\zeta_0} + \frac{n_+ l_+ + n_- l_-}{a} \right) \right) \tag{21}$$

From this equation we conclude that we need more assumptions in order to obtain length control. As noted in the main text the translational symmetry argument also applies here, so as a consequence x we assume that both the filaments extend to the nearest cell poles. Note that we now have $x_p(t) = l_-(t)$ and $\forall t \geq 0 : l_-(t) + l_+(t) = L$, the length of the filaments together cover the complete cell. The drag coefficients are now as follows:

$$\zeta_{A_-} = \zeta_0 \frac{n_- x_p(t)}{a}$$
$$\zeta_{A_+} = \zeta_0 \frac{n_+ \left(L - x_p(t) \right)}{a}$$

Again we together with 20 we insert this in eq. 19. With the assumption that both bundles consist of an equal number of filaments ($n_- = n_+ = n$), this leads to the following differential equation:

$$\left(\frac{\zeta_p}{\zeta_0} + \frac{nL}{a} \right) v_p(t) + 2 k_d x_p(t) - k_d L = 0$$

Solving this differential equation leads to proper positioning of one plasmid in the middle of a cell:

$$x_p(t) = \frac{L}{2} \left[1 - \exp \left(\frac{-k_d t}{\frac{\zeta_p}{\zeta_0} + \frac{nL}{a}} \right) \right] + x_p(0) \exp \left(\frac{-k_d t}{\frac{\zeta_p}{\zeta_0} + \frac{nL}{a}} \right) \quad \rightarrow \frac{L}{2} \;\; as \; t \rightarrow \infty \tag{22}$$

Lastly we investigate the possibility that one or two plasmids pull on plasmids with a high detachment rate. If τ is the average time a plasmid is connected to a polymer and stimulates the filament depolymerization and τ is low such that

$l(\tau) \approx l_0$ we may set t to zero in eq. 13. This means that the plasmid only feels the initial length in period that it is connected to the filament. Also we assume that the polymers extend to the cell poles because of the symmetry argument. In presence of one filament this simply leads to eq. 17. But in the presence of two opposing filaments A_- and A_+ extending to their respective poles, we may argue that due to short pulls in both directions the effective velocity of the plasmid will be the difference of the velocities because of the difference between the lengths l_- and l_+ and consequently the difference in drag coefficients. Now w.l.o.g. $l_- \leq l_+$ and since both polymers extend to the pole we obtain $l_- = x_p$ and $l_+ = L - x_p$. Taking the difference of the contributions arising from eq. 17 leads to eq. 2:

$$v_p(t) = \frac{k_d\,(L - x_p)}{\frac{\zeta_p}{\zeta_0} + \frac{(L-x_p)n_+}{a}} - \frac{k_d x_p}{\frac{\zeta_p}{\zeta_0} + \frac{x_p n_-}{a}}.$$

As denoted in the main text we assume that $n_- = n_+ = n$. In table 1 we list the velocities calculated with equations 17 and 2 for several drag ratios ζ_p/ζ_0. In the table parameters are set as follows: $k_d = 4s^{-1}$, $n = 1$ and $a = 2.5nm$. eq. 18 is the trajectory of the plasmid as it is being pulled by one filament that remains extended to the + pole. We require timely positioning, so that the position after $10min$ of pulling should be at least to mid cell ($1.0\mu m$). This limits the drag ratio to $\zeta_p/\zeta_0 \leq 10^3$ eq. 2 refers to the velocity difference due to two filaments that pull on a plasmid at $x_p = 0.1L_{min}$ while eq. 17 refers to the velocity when one filaments pulls on a plasmid at $x_p = 0.7L_{min}$ in the direction of the +pole. We require the velocity from 2 to be high compared to the one from 17. Also the absolute value of 2 and 17 with $x_p = 0.1L_{min}$ has to be high enough so that timely positioning can occur, this limits ζ_p/ζ_0 to $10^2 - 10^3$. The range of parameters is described in the main text and the according velocities lead to a similar conclusion: the velocities from 17 and 2 differ maximally by a factor of 1.8, which is not relevant enough to be the sole mechanism of plasmid partitioning.

ζ_p/ζ_0	10^6	10^5	10^4	10^3	10^2	10^1	10^0	10^{-1}
eq. A.1 $x_p(\mu m)$	0.0	0.0	0.1	0.5	1.5	1.9	2.0	2.0
eq. 18 $x_p(\mu m)$	0.0	0.0	0.4	1.6	2.0	2.0	2.0	2.0
eq. 2 $v_p(nm/s)$	0.006	0.063	0.592	3.445	4.336	0.974	0.110	0.011
eq. 17 $v_p(nm/s)$	0.002	0.024	0.234	1.935	7.059	9.600	9.959	9.996
eq. 2 : eq. 17	2.6	2.6	2.5	1.8	0.6	0.1	0.0	0.0

Table 1: For various drag coefficient ratios with eq. 18 the plasmid position after $10min$ is listed if one filament extending from the + pole is present and pulls on a plasmid, with initial position $x_p(0) = 0$. Also plasmid velocities are calculated with equations 17 and 2. eq. 2 refers to the velocity difference due to two opposing filaments that pull on a plasmid at $x_p = 0.1L_{min}$ while eq. 17 refers to the velocity when one filament pulls on a plasmid at $x_p = 0.7L_{min}$ extending from the +pole.

B Methods - Simulations

B.1 ParA filament pulling model with ParB levels determining the detachment rate

As we extended the program described in [1] with ParB dynamics we largely repeat here their explanation written in the supplementary material describing the ParA dynamics. In addition the program contains some extra functions on the ParB dynamics, dynamic cell growth and plasmid duplication. The program was written in C++. Kymographs and histograms were output to text files, which were imported in MATLAB to obtain the graphs shown in the main text.

The model was based on the following basic assumptions motivated by our experiments: (i) (ParA-ATP)$_2$ binds nonspecifically to the nucleoid surface. (ii) Once a critical cluster of (ParA-ATP)$_2$ has formed, cooperative ParA binding to the cluster edge becomes much more favored, with rapid bidirectional filament growth ensuing. (iii) When a ParA filament contacts a plasmid focus via ParB/parC, it attaches to the plasmid. (iv) The focus, via ParB/parC, then promotes hydrolysis of active ParA that causes this subunit to fall off the fil-

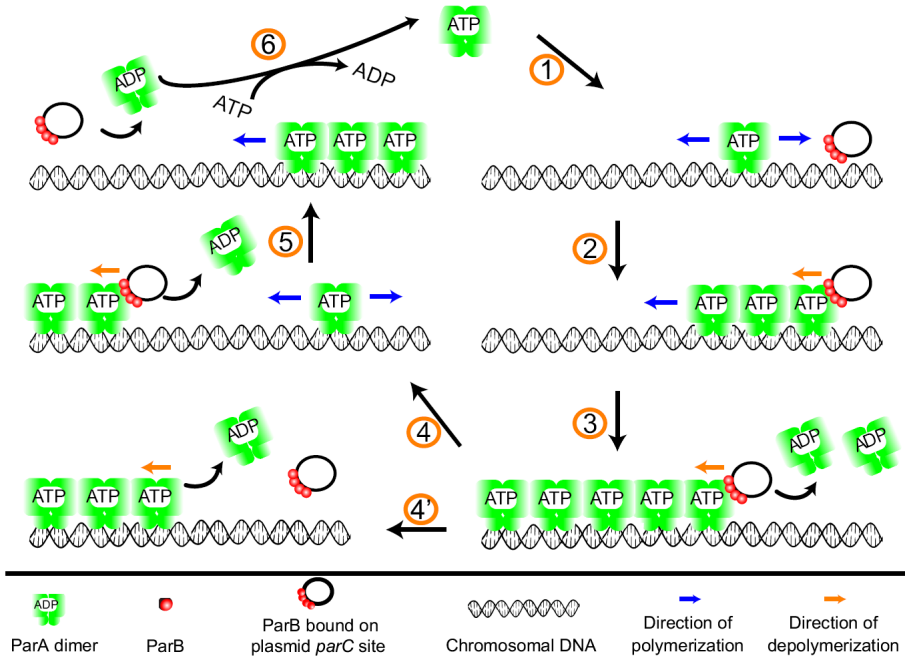

Figure 24: Schematic illustration of the ParA dynamics in the simulations [1]. In the text of this section the different steps are explained in detail.

ament end, thereby generating filament shrinkage. (v) The focus is dragged along with the shrinking filament before spontaneously detaching. (vi) Regardless of focus attachment, once a filament has contacted a focus, the filament will continue to shrink until it has entirely disappeared. (vii) The inactive form of ParA, $(\text{ParA-ADP})_2$, in the cytoplasm undergoes nucleotide exchange in the cytoplasm to $(\text{ParA-ATP})_2$, which is again able to bind to the nucleoid.

We implemented a 1D lattice, stochastic version of the molecular model outlined above and in the main text. The rules for our initial model were as follows (also see fig. 24): ParA-ATP molecules in the cytoplasm were able, at each time step, to bind to any unoccupied nucleoid lattice site. If binding occurred at a site where both neighboring sites were unoccupied, or at a site next to a filament consisting of less than six molecules (excluding the newly bound molecule), then the process occurred with probability $\frac{k_1 A \mathrm{d}t}{L}$, where A was the number of cytoplasmic $(\text{ParA-ATP})_2$ molecules, k_1 a binding rate, dt the time step and L the cell length expressed as the number of binding sites (we used a lattice spacing

$\mathrm{d}x = 2.5nm$).

For filaments of six molecules or less, a $(\text{ParA-ATP})_2$ molecule could undergo spontaneous hydrolysis and dissociate from either end of the filament, with each event occurring with probability $k_2\ \mathrm{d}t$. Once a filament of six $(\text{ParA-ATP})_2$ molecules had formed, then subsequent cooperative binding to neighboring unoccupied lattice sites occurred at a much increased probability $\frac{k_3 A \mathrm{d}t}{L}$, whereas dissociation from filament ends was prohibited. These rules implemented a nucleation elongation model of bidirectional $(\text{ParA-ATP})_2$ filament polymerization with a critical nucleus of six molecules (although the precise number of molecules in the critical nucleus is unimportant).

Ends of the $(\text{ParA-ATP})_2$ filaments were allowed to grow stochastically until they either (i) reached one of the nucleoid poles, where polymerizing growth at that end ceased, or (ii) occupied a lattice site adjacent to a ParB/parC centromeric complex. In the latter case, filament polymerization at that end also ceased, and the ParB/parC complex was assumed to attach to the filament and initiate filament contraction. At each time step, the $(\text{ParA-ATP})_2$ molecule on a contracting filament end was allowed to undergo ParB-stimulated hydrolysis and unbind with probability $k_4 \mathrm{d}t$. At the same time, the plasmid focus was pulled along by one lattice site to the left or right, as appropriate. Whenever $(\text{ParA-ADP})_2$ unbinding occurred, we also allowed for a probability p_5 for the plasmid focus to detach from the filament. This probability depends on the ParB number at the plasmid. See below for more details on the rules for ParB and how p_5 is calculated.

Regardless of plasmid focus attachment, we assumed that the filament continued to shrink until it had entirely disappeared following first contact with a site occupied by ParB/parC. Finally, when two filaments come in contact with one another, we merge the filaments into a single one only if both the touching ends are growing, not contracting. During the course of the simulations, we kept track of the positions and lengths of $(\text{ParA-ATP})_2$ filaments, as well as the status (growing or shrinking) of the filament ends and the occupancy of

each individual lattice site. To reduce the computational demands of the simulations, we assumed that cytoplasmic diffusion was sufficiently fast that the ParA molecules in the cytoplasm were always well mixed. We did not therefore track the positions of ParA subunits in the cytoplasm, but only monitored their overall number. We also assumed that nucleotide exchange of ParA in the cytoplasm from $(\text{ParA-ADP})_2$ to $(\text{ParA-ATP})_2$ (that could subsequently rebind to the nucleoid) was slow compared with the timescales of cytoplasmic diffusion. Consequently, we did not model the exchange process, but once an unbinding reaction occurred, we set up a timer for that $(\text{ParA-ADP})_2$ subunit. After a waiting time τ_{WT} we considered it activated again, so that A was increased with one.

We continue with the ParB dynamics (also see fig. 25): the total number

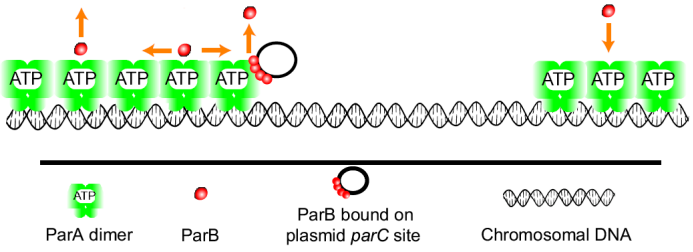

Figure 25: Schematic illustration of the ParB dynamics in the simulations adjusted from [1]. In the text of this section the different steps are explained in detail.

of ParB in the systems is assumed to scale with the plasmid copy number n_p: $B_{total} = B_0\ n_p$. Again we do not model the cytoplasmic ParB diffusion but assume it is constant as it does not change rapidly since the binding rates of ParB are low compared to cytoplasmic diffusion. B denotes the number of cytoplasmic ParB units and at every update round when a ParA site is occupied a ParB can bind to it with probability $\frac{k_7 B \mathrm{d}t}{L}$, likewise it can bind directly to a plasmid with probability $\frac{k_9 B \mathrm{d}t}{L}$. A ParB can also detach from a ParA site with probability $k_7 \mathrm{d}t$ and from the plasmid with probability $k_9 \mathrm{d}t$.

If a plasmid is attached to a ParA filament, we assumed that the plasmid absorbs

the sliding ParB molecules instantaneously. This approximation is valid in the limit of rapid diffusion compared to changes in the length of ParA filaments. We also did simulations in which the probability distribution of ParB diffusion was calculated after time dt and sampled the new positions of the ParB molecules, but this did not change the results of the simulations (results not shown). If two plasmids were connected to a polymer at either end, either the ParB had a probability of $\frac{1}{2}$ to be absorbed by a particular plasmid.

The calculation of the detachment probability was as follows: if the ParB number that is bound to a plasmid B_p exceeds a threshold T, $p_5 = 0$. Otherwise it is nonzero and follows a hill curve with coefficient 2 and half maximum 1.5: $p_5 = \frac{1.5^2}{1.5^2 + \mathrm{B_p}^2}$. The precise shape does not matter for the qualitative behaviour of the system as long as it decreases from one at $B_p = 0$ to zero at $B_p = \mathrm{T}$.

At the beginning of each update round in the simulation we checked whether an inactive cytoplasmic ParA unit was ready to become the (ParA-ATP)$_2$ form again. Subsequently the renewal of firstly ParA and secondly ParB distributions were performed. Finally we allowed for possible plasmid duplication events and cell growth either at fixed time intervals or with different rates. Parameter values that were used are: $k_1 = 0.3 \#molecule^{-1} \cdot \#bindingsites \cdot s^{-1}$, $k_2 = 0.2 s^{-1}$, $k_3 = 50\ \#molecule^{-1} \cdot \#bindingsites \cdot s^{-1}$, $k_4 = 1 s^{-1}$, $\mathrm{T} = 6$, $k_7 = 4 \cdot 10^{-4} \mathrm{T}\ \#molecule^{-1} \cdot \#bindingsites \cdot$, $k_8 = 0.1 s^{-1}$, $k_9 = k_7$, $k_{10} = k_8$, $\tau_{\mathrm{WT}} = 3333 \mathrm{d}t = 30 s$, $B_0 = 500$ and the total number of ParA subunits was equal to the number of binding sites at any time, this means that the ParA copy number scales with the cell size.

B.2 Outline of the Gillespie algorithm

	Set parameters and initial values.
	Output parameters to logfile.
	Define reactions and reactants.
	Set initial propensities.
Do →	If ($t >= t_{growth}$): Cell growth, $t_{growth} = t_{growth} + \mathrm{d}t_{growth}$
	If ($t >= t_{dup}$): Create plasmid, $t_{dup} = t_{dup} + \mathrm{d}t_{dup}$
	If ($t >= t_{dup}$): Output to file, (output to bitmap), $t_{out} = t_{out} + \mathrm{d}t_{out}$
↑ ↓	Generate $r_1 \in (0, 1)$: $\tau = \frac{1}{p_{sum}} \log\left[\frac{1}{r_1}\right]$.
	Generate random numbers to determine new reaction.
	Perform reaction.
	Update affected propensities, calculate p_{sum}
←	Update timers for inactive ParA units, update affected propensities.
While($t <$ Time)	$t = t + \tau$.
	Output histograms, (create movie).

Table 2: Schematic outline of the Gillespie algorithm implementation that was used for the simulations discussed further in sections B.3,B.4, B.5 and B.6. Only the different reactions, parameters, reactants and calculations of the propensities (probability per unit time) are different among the various simulations. All other functions in the C++ code remained the same. Time denotes the total amount of simulated time. r_1 is a generated random number, for all simulations we used the pseudorandom number generator Mersenne Twister. p_{sum} is the sum of the propensities of all possible reactions in the system. $\mathrm{d}t_{growth}$, $\mathrm{d}t_{dup}$ and $\mathrm{d}t_{out}$ are the time interval in between cell growth, plasmid duplication and data output respectively and t_{growth}, t_{dup} and t_{out} indicate the time points of the first coming respective events. The steps on the right of the do-while statement occur inside the loop and are repeated until t, the current time of the simulation at least equals Time. The timer update is a deterministic activation of ParA units after 30s. In the ParA slide simulation this feature was replaced by a stochastic version. See appendix B.6 for more information.

B.3 Biased diffusion model

The features of the Gillespie algorithm that are different for the specific simulations are described in this and the following three sections. They contain the reactions, reactants, parameters and reactions types listed in tables. The different reaction types determine how the propensities are calculated which are explained as well. Table 3 shows the reactions used in the biased diffusion simulations and table 4 explains the determination of their propensities.

Name	Reaction	Parameter(s)	Reaction Type
Nucleoid binding reaction	$\mathrm{A_{cyto}} \rightarrow \mathrm{ParA}[i]$ $i \in \{0..l-1\}$	$\frac{k_{on}}{l}$	first order
Spontaneous hydrolysation	$\mathrm{ParA}[i] \rightarrow \mathrm{Timer}$ $i \in \{0..l-1\}$	k_{off}	first order
ParA diffusion	$\mathrm{ParA}[k] \rightarrow \mathrm{ParA}[k+1]$	$\frac{D_A}{\mathrm{d}x^2}$	first order
	$\mathrm{ParA}[k+1] \rightarrow \mathrm{ParA}[k]$		
	$k \in \{0..l-2\}$		
Plasmid diffusion	$\mathrm{P}[k] \rightarrow \mathrm{P}[k+1]$	$\frac{D_p}{\mathrm{d}x^2}$	biased diffusion
	$\mathrm{P}[k+1] \rightarrow \mathrm{P}[k]$		
	$k \in \{0..l-2\}$		
Stimulated hydrolysation	$\mathrm{P}[i] + \mathrm{ParA}[i] \rightarrow \mathrm{P}[i] + \mathrm{Timer}$	k_{AB}	second order
	$i \in \{0..l-1\}$		

Table 3: Different reactions used in the biased diffusion simulations. l is the number of sites, L the nucleoid length and $\mathrm{d}x$ the gridsize: $l = \frac{L}{\mathrm{d}x}$.

Reaction type (rate constant, reactant number(s))	Calculation of propensity p
first order (k, r)	$p = k \cdot r$
second order $(k, \mathrm{P[i]}, \mathrm{ParA}[i])$	$p = k \cdot \frac{\mathrm{P}[i]}{\mathrm{d}x} \cdot \mathrm{ParA}[i]$
biased diffusion$(k, \mathrm{P}[i], \mathrm{ParA}[i])$	if$(\mathrm{ParA}[i] < 1)$: $p = k \cdot \mathrm{P}[i]$
	else if$(\mathrm{ParA}[i] > 1)$: $p = 0$
	else: $p = \frac{k}{2} \cdot \mathrm{P}[i]$

Table 4: Calculation of propensities for the reactions in the biased diffusion simulations. k is the relevant rate constant either in units of s^{-1} or $s^{-1} \cdot molecules^{-1} \cdot m$ for respectively first and second order reactions. The biased diffusion reaction resembles a threshold reaction, which could be seen as a cooperative reaction with hill coefficient ∞ and half maximum of one ParA at the site.

B.4 ParA oligomer pulling model

Name	Reaction	Parameter(s)	Reaction Type
Nucleoid binding reaction	$A_{\text{cyto}} \rightarrow \text{ParA}[i]$, $i \in \{0..l-1\}$	$\frac{k_{on}}{l}$	first order
Spontaneous hydrolysation	$\text{ParA}[i] \rightarrow \text{Timer}$, $i \in \{0..l-1\}$	k_{off}	first order
ParA diffusion	$\text{ParA}[k] \rightarrow \text{ParA}[k+1]$	$\frac{D_A}{\mathrm{d}x^2}$	first order
	$\text{ParA}[k+1] \rightarrow \text{ParA}[k]$		
	$k \in \{0..l-2\}$		
Plasmid pulling	$\text{P}[k] + \text{ParA}[k+1] \rightarrow \text{P}[k+1] +$ Timer	k_{AB}	second order
	$\text{P}[k+1]+\text{ParA}[k] \rightarrow \text{P}[k]+\text{Timer}$		
	$k \in \{0..l-2\}$		

Table 5: Different reactions used in the oligomer pulling simulations. l is the number of sites, L the nucleoid length and $\mathrm{d}x$ the gridsize: $l = \frac{L}{\mathrm{d}x}$. For reactions of the simulations in which plasmid diffusion is allowed we refer to the next section in the appendix.

Reaction type (rate constant, reactant number(s))	Calculation of propensity p
first order (k, r)	$p = k \cdot r$
second order $(k, \text{P}, \text{ParA})$	$p = k \cdot \frac{\text{P}}{\mathrm{d}x} \cdot \text{ParA}$

Table 6: Calculation of propensities for the reactions in the oligomer pulling simulations. k is the relevant rate constant either in units of s^{-1} or $s^{-1} \cdot molecules^{-1} \cdot m$ for respectively first and second order reactions. The pulling occurs between a plasmid and a ParA oligomer at neighboring sites. In different simulations $\mathrm{d}x$ was varied from $5-50nm$ which does not render this rule artificial as the size of the plasmid is itself on the order of $10^2 nm$.

B.5 Linear self organization of ParA

Most reactions in this system are again first or second order reaction although the diffusive reactions of ParA oligomers involve now Head-Tail (affinity H) and lateral "side" interactions (affinity S). The theory of the interactions of ParA oligomers in absence of plasmids are explained superficially in section 2.5. Here we describe the calculation of the propensities for the diffusive reactions. In the spatial Gillespie algorithm the sites indexed by coordinates on the cylinder are the states and the reactions are the movement of an oligomer from one site to another. To calculate the propensity of the reaction we sum over the propensities of every oligomer at that site to overcome the energy barrier that is necessary to make the jump. Since the Gillespie algorithm only retains the number of oligomers at a site, this makes the oligomers indistinguishable, but the collection of energy levels of all oligomers at a particular site are uniquely defined by the rules described above. If such an energy level E of an oligomer has $E < 0$, this oligomer must have associated bonds. In that case if the new site has no oligomers, all bonds have to be broken so $E^{\ddagger} = 0$, equal to the free diffusive energy level. On the other hand if the new site does have at least one oligomer, some lateral interaction remains during the movement so the energy barrier is lowered: $E^{\ddagger} = -S$ or $E^{\ddagger} = -2S$ depending on the number of current lateral bonds. If no bonds existed (free diffusion), $E^{\ddagger} = 0$. We set F equal to the free diffusive rate. eq. 9 determines the propensities of single oligomers overcoming the energy barrier and moving to a neighboring site and as noted above these propensities are summed over to obtain the propensity for a reaction to occur in the Gillespie algorithm.

Since the simulations are now done on a two dimensional surface the sites have two indices (i, j), the first one being the coordinate along the long axis of size L. The number of sites along that axis is $l = \frac{\mathrm{L}}{\mathrm{d}x_{\parallel}}$. Likewise the circumference has sites $c = \frac{\mathrm{C}}{\mathrm{d}x_{\perp}}$ with $\mathrm{C} = 3.2\mu m$ the circumference of a cell. There are two new states of the ParA oligomers in the presence of plasmids: APm indicates an oligomer bound on the $-$side of the plasmid (therefore it cannot be at site the right edge of the nucleoid at $i = l - 1$) due to the volume of the plasmid) and APp an oligomer bound on the +side of the plasmid (cannot be at $i = 0$).

We assume in the calculation of the diffusion rates that ParA will always form Head-Tail affinities preferentially over both APm and APp, secondly if there are both APm and APp at a site then the APm will form a Head-Tail interaction with the − neighbor and APp with the + neighbor. This determines the rules as written down below in pseudo code. Lastly the pulling reaction occurs

Name	Reaction	Parameter(s)	Reaction Type
Nucleoid binding reaction	$A_{cyto} \rightarrow ParA[i][j]$	$\frac{k_{c0}}{ls}, \frac{k_{c1}}{ls}$	cooperative binding
Spontaneous hydrolysation	$ParA[i][j] \rightarrow Timer$	k_{off}	first order
	$i \in \{0..l-1\}, j \in \{0..s-1\}$		
Plasmid attachment	$P[k][j] + ParA[k+1][j] \rightarrow APp[k+1][j]$	k_{at}	second order
	$P[k+1][j] + ParA[k][j] \rightarrow APm[k][j]$	k_{at}	second order
	$k \in \{0..l-2\}$		
Stimulated hydrolysation	$APm[k][j] \rightarrow P[k(+1)][j] +$ Timer $k \in \{0..l-2\}$	k_{pull}	first order
	$APp[k][j] \rightarrow P[k(-1)][j] +$ Timer	k_{pull}	first order
	$k \in \{1..l-1\}$		
ParA diffusion	$ParA[k][j] \rightarrow ParA[k+1][j]$	$\frac{D_A}{dx_\parallel^2}$,	oligomer interaction
(along long axis)	$ParA[k+1][j] \rightarrow ParA[k][j]$	H,S,F	
(along circumference)	$ParA[i][j] \rightarrow ParA[i][(j+1)\%c]$	$\frac{D_A}{dx_\perp^2}$,	oligomer interaction
	$ParA[i][(j+1)\%c] \rightarrow ParA[i][j]$	H,S,F	
Plasmid diffusion	$P[k][j] \rightarrow P[k+1][j]$	$\frac{D_p}{dx_\parallel^2}$	first order
(along long axis)	$P[k+1][j] \rightarrow P[k][j]$		
(along circumference)	$P[i][j] \rightarrow P[i][(j+1)\%c]$	$\frac{D_p}{dx_\perp^2}$	first order
	$P[i][(j+1)\%c] \rightarrow P[i][j]$		
APm diffusion	$APm[k][j] \rightarrow APm[k+1][j]$	$\frac{\min(D_A,D_p)}{dx_\parallel^2}$,	oligomer interaction
(along long axis)	$APm[k+1][j] \rightarrow APm[k][j]$	H,S,F	
	$k \in \{0..l-3\}$		
(along circumference)	$APm[k][j] \rightarrow APm[k][(j+1)\%c]$	$\frac{\min(D_A,D_p)}{dx_\perp^2}$,	oligomer interaction
	$APm[k][(j+1)\%c] \rightarrow APm[k][j]$	H,S,F	
	$k \in \{0..l-2\}$		
APp diffusion	$APp[k][j] \rightarrow APp[k+1][j]$	$\frac{\min(D_A,D_p)}{dx_\parallel^2}$,	oligomer interaction
(along long axis)	$APp[k+1][j] \rightarrow APp[k][j]$	H,S,F	
	$k \in \{1..l-2\}$		
(along circumference)	$APp[k][j] \rightarrow APp[k][(j+1)\%c]$	$\frac{\min(D_A,D_p)}{dx_\perp^2}$,	oligomer interaction
	$APp[k][(j+1)\%c] \rightarrow APp[k][j]$	H,S,F	
	$k \in \{1..l-1\}$		

Table 7: Different reactions used in the self organization simulations. l is the number of sites along the long axis, L, and $dx_\parallel$ the gridsize: $l = \frac{L}{dx_\parallel}$. $C = 3.2\mu m$ is the circumference of the nucleoid with a gridsize $dx_\perp$, c is the number of sites along the circumference: $c = \frac{C}{dx_\perp}$

Reaction type (rate constant, reactant number(s))	Calculation of propensity p
first order (k, r)	$p = k \cdot r$
second order (k, r, s)	$p = k \cdot \frac{r}{\mathrm{d}x_{\parallel}\mathrm{d}x_{\perp}} \cdot s$
cooperative binding	$p = A_{cyto} \cdot$
$(\frac{k_{c0}}{ls}, \frac{k_{c1}}{ls}, A_{cyto}, \mathrm{ParA}[i][j], \mathrm{APm}[i][j], \mathrm{APp}[i][j])$	$\left(\frac{k_{c0}}{ls} + \frac{k_{c1}}{l} \frac{(\mathrm{ParA}[i][j]+\mathrm{APm}[i][j]+\mathrm{APp}[i][j])^2}{(\mathrm{ParA}[i][j]+\mathrm{APm}[i][j]+\mathrm{APp}[i][j])^2+1}\right)$

Table 8: Calculation of propensities for the reactions in the self organization simulations. k is the relevant rate constant either in units of s^{-1} or $s^{-1} \cdot molecules^{-1} \cdot m^2$ for respectively first and second order reactions. The cooperative binding reaction has a hill coefficient of 2 and a half maximum of 1. Cooperative binding of ParA is reported experimentally [2]. The function that determines the diffusion propensities is shown on the next page.

with a success factor $0 < sf \leq 1$. This means that whenever the stimulated hydrolysation reaction occurs at site i, with probability sf the plasmid is pulled to the site i where the AP complex was located. If the pulling event was not successful, the plasmid remains at the $i+1$ for APm and $i-1$ for APp. As long as the plasmid is bound to a complex at site i (APm[i] or APp[i]), we consider the position of the plasmid to be $i+1$ and $i-1$ respectively, only after the depolymerization the plasmid can changed to site i.

oligomer interaction for diffusion away from site (i,j)

$p = 0; E_a = 0$;(p is propensity to be calculated, r is reactant, either ParA, APm or APp

Am_{oc} = number of "occupied" ParA oligomers at site (i-1,j)

which are unavailable for Head-Tail interactions.

For ParA:0, for APm[i][j]: ParA[i][j]

and for APp[i][j]: ParA[i][j] + APm[i][j]

Ap_{oc} = number of "occupied" Head-Tail interactions on the + side.

For ParA: 0, for APm[i][j]: ParA[i][j] + APp[i][j] and for APp[i][j]: ParA[i][j]

A = ParA[i][j] + APm[i][j] + APp[i][j], total number of oligomers at site.

A_{new} is the number of ParA oligomers at the "new" site where the diffusion reaction will lead to.

k_d is the free diffusive rate as listed in table 7.

$if(A == 1)$

$freq = k_d$;

$E = 0$; (no lateral interaction)

$E = -H \cdot \min(Am, 1)$;

$E = E - H \cdot \min(Ap, 1)$;

$if(E < 0)$:

$freq = F$;

$if(A_{new} > 0)$

$E_a = -L$;

$p = freq \cdot \exp(E - E_a)$;

$elseif(A == 2)$

$freq = F$;

$if(A_{new} > 0)$

$E_a = -L$; (energy barrier is lowered)

$for(i = 0; i < r; i++)$

$E = -L$; (lateral interaction of ParA)

$if(Am > 0)$

$E = E - H$;

$Am--$;

$if(Ap > 0)$

$E = E - H$;

$Ap--$;

$p = p + freq \cdot \exp(E - E_a)$;

$else$ (more than two oligomers at site)

$freq = F$;

$if(Anew > 0)$

$Ea = -2L$;

$for(i = 0; i < r; i++)$

$E = -2L$; (lateral interaction of ParA)

$if(Am > 0)$

$E = E - H$;

$Am--$;

$if(Ap > 0)$

$E = E - H$;

$Ap--$;

$p = p + freq \cdot \exp(E - Ea)$;

B.6 ParA filament pulling model with ParA sliding

The ParA slide simulations have certain microscopic differences from the previous simulation: we assume the ParAs exhibit a rather strong affinity B for a nucleoid which slows down diffusion along the nucleoid considerably. but once a site has a ParA subunit bound to it, the other possible ParAs at that site do not sense the interaction with the DNA so that they automatically become a new species: ParA that can slide along the filaments (AS). On Top of that we assume that the Head-Tail affinity is very strong so that we obtain polymerization in the sense that if two neighboring ParAs are present, the diffusion rate of both is set to zero due to a strong head tail interaction. Spontaneous depolymerization can only occur at the tip ends of the ParA polymers. This induces ParA polymer formation. Once a ParA at site disappears some how, if there is AS present at the site, one of them automatically becomes a ParA due to the affinity for the nucleoid. Plasmids can bind to ParA to form APm or APp and depolymerize again and induce plasmid motion with success factor sf. Plasmid diffusion is set to zero in these simulation and the system is one dimensional again. AS cannot unbind, although this seems artificial, it is reasonable since we put the diffusion constant of the sliding molecules high so that they will find an empty site and became ParA again before they can unbind. The reactions and propensities are shown in table 9 and 10. In this simulation we made Timer a separate state rather than extracting adding ParA back into the cytoplasm after the waiting time deterministically. After hydrolysation the ParA becomes Timer and with rate $1/\tau_{\mathrm{WT}}$, Timer is converted into cytoplasmic ParA which is capable of binding the nucleoid.

Name	Reaction	Parameter(s)	Reaction Type
Nucleoid binding reaction	$\mathrm{A_{cyto}} \rightarrow \mathrm{ParA}[i]$	$\frac{k_{c0}}{l}, \frac{k_{c1}}{l}$	cooperative binding
Spontaneous hydrolysation	$\mathrm{ParA}[i] \rightarrow \mathrm{Timer}$	k_{off}	spontaneous unbind
	$i \in \{0..l-1\}$		
Plasmid attachment	$\mathrm{P}[k] + \mathrm{ParA}[k+1] \rightarrow \mathrm{APp}[k+1]$	k_{at}	second order
	$\mathrm{P}[k+1] + \mathrm{ParA}[k] \rightarrow \mathrm{APm}[k]$	k_{at}	second order
	$k \in \{0..l-2\}$		
Stimulated hydrolysation	$\mathrm{APm}[k] \rightarrow \mathrm{P}[k(+1)] + \mathrm{Timer}$	k_{pull}	first order
	$k \in \{0..l-2\}$		
	$\mathrm{APp}[k] \rightarrow \mathrm{P}[k(-1)] + \mathrm{Timer}$	k_{pull}	first order
	$k \in \{1..l-1\}$		
ParA diffusion	$\mathrm{ParA}[k] \rightarrow \mathrm{ParA}[k+1]$	$\frac{D_A}{\mathrm{d}x_\parallel^2}, B$	ParA diffusion
	$\mathrm{ParA}[k+1] \rightarrow \mathrm{ParA}[k]$		
AS diffusion	$\mathrm{AS}[k] \rightarrow \mathrm{AS}[k+1]$	$\frac{D_A}{\mathrm{d}x_\parallel^2}$	first order
	$\mathrm{AS}[k+1] \rightarrow \mathrm{AS}[k]$		
ParA activation	$\mathrm{Timer} \rightarrow \mathrm{A_{cyto}}$	$1/\tau_{\mathrm{WT}}$	first order

Table 9: Different reactions used in the ParA sliding simulations. l is the number of sites, L the nucleoid length and $\mathrm{d}x_\parallel$ the gridsize: $l = \frac{L}{\mathrm{d}x_\parallel}$.

Reaction type (rate constant, reactant number(s))	Calculation of propensity p
first order (k, r)	$p = k \cdot r$
second order $(k, \mathrm{P}, \mathrm{A})$	$p = k \cdot \frac{\mathrm{P}}{\mathrm{d}x_\parallel} \cdot \mathrm{A}$
cooperative binding	if($\mathrm{ParA}[i] + \mathrm{APm}[i] + \mathrm{APp}[i] = 0$): $p = \frac{k_{c0}}{l} \cdot \mathrm{A_{cyto}}$
$(\frac{k_{c0}}{l}, \frac{k_{c1}}{l}, A_{cyto}, \mathrm{ParA}[i][j], \mathrm{APm}[i][j], \mathrm{APp}[i][j])$	else: $p = \frac{k_{c1}}{l} \cdot \mathrm{A_{cyto}}$
spontaneous unbind	if(any of ParA,APm and APp
(k_{off},neighboring ParA,APm and APp)	are present on *both* sides): $p = 0$;
	else: $p = k_{off}$;
ParA diffusion	if(any of ParA,APm and APp
(k,neighboring ParA,APm and APp)	are present on *either* side): $p = 0$;
	else: $p = k \exp(-B)$;

Table 10: Calculation of propensities for the reactions in the ParA sliding simulations. k is the relevant rate constant either in units of s^{-1} or $s^{-1} \cdot molecules^{-1} \cdot m$ for respectively first and second order reactions and ParA diffusion. The cooperative binding needs only a constant k_{c1} because the amount of bound ParA present at a site when this formula is used equals one, so introducing a hill coefficient and a half maximum would add a constant factor to the binding rate. Cooperativity due to AS at a site is not taken into account, since we assume that it slides rapidly to the tip.

References

[1] S. Ringgaard, J. van Zon, M. Howard, and K. Gerdes, "Movement and equipositioning of plasmids by ParA filament disassembly," *Proc Natl Acad Sci USA*, vol. 106, pp. 19369–19374, Nov 2009.

[2] A. G. Vecchiarelli, Y. W. Han, X. Tan, M. Mizuuchi, R. Ghirlando, C. Biertümpfel, B. E. Funnell, and K. Mizuuchi, "ATP control of dynamic P1 ParA-DNA interactions: a key role for the nucleoid in plasmid partition," *Mol Microbiol*, vol. 78, pp. 78–91, Oct 2010.

[3] B. Alberts, *Molecular Biology of the Cell*. Other, 5 ed., Nov 2007.

[4] K. Gerdes, M. Howard, and F. Szardenings, "Pushing and Pulling in Prokaryotic DNA Segregation," *Cell*, vol. 141, pp. 927–942, June 2010.

[5] M. Howard, A. D. Rutenberg, and S. de Vet, "Dynamic compartmentalization of bacteria: accurate division in E. coli," *Phys Rev Lett*, vol. 87, pp. 278102–278102, Dec 2001.

[6] T. D. Dunham, W. Xu, B. E. Funnell, and M. A. Schumacher, "Structural basis for ADP-mediated transcriptional regulation by P1 and P7 ParA," *EMBO J*, vol. 28, pp. 1792–1802, Jun 2009.

[7] M. A. J. Roberts, G. H. Wadhams, K. Hadfield, S. Tickner, and J. P. Armitage, "Preprint: A ParA-like protein uses non-specific chromosomal DNA binding to partition protein complexes." Feb 2011.

[8] T. Hatano and H. Niki, "Partitioning of P1 plasmids by gradual distribution of the ATPase ParA," *Mol Microbiol*, vol. 78, pp. 1182–1198, Dec 2010.

[9] G. Ebersbach and K. Gerdes, "The double par locus of virulence factor pB171: DNA segregation is correlated with oscillation of ParA," *Proc Natl Acad Sci USA*, vol. 98, pp. 15078–15083, Dec 2001.

[10] S. Ringgaard, G. Ebersbach, J. Borch, and K. Gerdes, "Regulatory cross-talk in the double par locus of plasmid pB171," *J Biol Chem*, vol. 282, pp. 3134–3145, Feb 2007.

[11] S. Ringgaard, J. Löwe, and K. Gerdes, "Centromere pairing by a plasmid-encoded type I ParB protein," *J Biol Chem*, vol. 282, pp. 28216–28225, Sep 2007.

[12] S. R. Thompson, G. H. Wadhams, and J. P. Armitage, "The positioning of cytoplasmic protein clusters in bacteria," *Proc Natl Acad Sci USA*, vol. 103, pp. 8209–8214, May 2006.

[13] G. Ebersbach and K. Gerdes, "Bacterial mitosis: partitioning protein ParA oscillates in spiral-shaped structures and positions plasmids at mid-cell," *Mol Microbiol*, vol. 52, pp. 385–398, Apr 2004.

[14] M. B. Elowitz, M. G. Surette, P.-E. Wolf, J. B. Stock, and S. Leibler, "Protein Mobility in the Cytoplasm of Escherichia coli," *J. Bacteriol.*, vol. 181, pp. 197–203, Jan. 1999.

[15] G. Ebersbach, S. Ringgaard, J. Moller-Jensen, Q. Wang, D. J. Sherratt, and K. Gerdes, "Regular cellular distribution of plasmids by oscillating and filament-forming ParA ATPase of plasmid pB171," *Mol Microbiol*, vol. 61, pp. 1428–1442, Sep 2006.

[16] C. Machón, T. J. Fothergill, D. Barillà, and F. Hayes, "Promiscuous stimulation of ParF protein polymerization by heterogeneous centromere binding factors," *J Mol Biol*, vol. 374, pp. 1–8, Nov 2007.

[17] M. Sengupta, H. J. Nielsen, B. Youngren, and S. Austin, "P1 plasmid segregation: accurate redistribution by dynamic plasmid pairing and separation," *J Bacteriol*, vol. 192, pp. 1175–1183, Mar 2010.

[18] V. Sourjik and J. P. Armitage, "Spatial organization in bacterial chemotaxis," *EMBO J*, vol. 29, pp. 2724–2733, Aug 2010.

[19] C. S. Campbell and R. D. Mullins, "In vivo visualization of type II plasmid segregation: bacterial actin filaments pushing plasmids," *J Cell Biol*, vol. 179, pp. 1059–1066, Dec 2007.

[20] O. Rodionov, M. Lobocka, and M. Yarmolinsky, "Silencing of genes flanking the P1 plasmid centromere," *Science*, vol. 283, pp. 546–549, Jan 1999.

[21] V. Varga, J. Helenius, K. Tanaka, A. A. Hyman, T. U. Tanaka, and J. Howard, "Yeast kinesin-8 depolymerizes microtubules in a length-dependent manner," *Nat Cell Biol*, vol. 8, pp. 957–962, Sep 2006.

[22] P. C. Blainey, A. M. van Oijen, A. Banerjee, G. L. Verdine, and X. S. Xie, "A base-excision DNA-repair protein finds intrahelical lesion bases by fast sliding in contact with DNA," *Proc Natl Acad Sci USA*, vol. 103, pp. 5752–5757, Apr 2006.

[23] I. A. Berlatzky, A. Rouvinski, and S. Ben-Yehuda, "Spatial organization of a replicating bacterial chromosome," *Proc Natl Acad Sci USA*, vol. 105, pp. 14136–14140, Sep 2008.

[24] P. A. Wiggins, K. C. Cheveralls, J. S. Martin, R. Lintner, and J. Kondev, "Strong intranucleoid interactions organize the Escherichia coli chromosome into a nucleoid filament," *Proc Natl Acad Sci USA*, vol. 107, pp. 4991–4995, Mar 2010.

[25] T. Sugawara and K. Kaneko, "Preprint: Spatial order induced by entropic force under chemical gradient." Nov 2010.

[26] I. Golding and E. C. Cox, "Physical Nature of Bacterial Cytoplasm," *Phys Rev Lett*, vol. 96, pp. 098102+, Mar. 2006.

[27] D. T. Gillespie, "Exact stochastic simulation of coupled chemical reactions," *The Journal of Physical Chemistry*, vol. 81, no. 25, pp. 2340–2361, 1977.

[28] A. Slepoy, A. P. Thompson, and S. J. Plimpton, "A constant-time kinetic Monte Carlo algorithm for simulation of large biochemical reaction networks," *The Journal of Chemical Physics*, vol. 128, no. 20, p. 205101, 2008.

[29] M. Howard and K. Gerdes, "What is the mechanism of ParA-mediated DNA movement?," *Mol Microbiol*, vol. 78, pp. 9–12, Oct 2010.